Pair Spectra and the Magnetic Properties of Co^{2+} in Double Nitrate Crystals*

J. W. CULVAHOUSE AND DAVID P. SCHINKE†
Department of Physics and Astronomy, The University of Kansas, Lawrence, Kansas 66044
(Received 2 June 1969)

Measurements of the pair spectra of Co^{2+} ions in $La_2Zn_3(NO_3)_{12}\cdot 24H_2O$ and $La_2Mg_3(NO_3)_{12}\cdot 24H_2O$ are reported and interpreted. The two types of sites for divalent ions (two X sites and one Y site in the unit cell) lead to spectra corresponding to pairs of similar and dissimilar anisotropic ions. The theory for the interpretation of these spectra in terms of a phenomenological spin-spin interaction is given and used to show that there are only two large interactions: the nearest-neighbor X-X and nearest-neighbor X-Y. All other interactions are small and dipolar. The nondipolar part of the interactions are shown to be of the form $K_{\parallel}S_1^zS_2^z+K_{\perp}(S_1^xS_2^x+S_1^yS_2^y)$. This form is given by the projection of isotropic exchange between ionic spins onto the effective spin states. This model gives a value for $K_{\parallel}/K_{\perp}$ which agrees well with the experimental value for the X-Y but not for the X-X. It is shown that the validity of isotropic exchange between ionic spins hinges upon the involvement of only e_g orbitals in the exchange process, and that this is probable for the X-Y pairs because of the hydrogen bonding between the complexes. Similar bonding does not exist between the X complexes. In a general way this accounts for the fact that the nondipolar part of the X-X interaction is smaller than that for the X-Y despite the interionic separations of 4.99 and 7.14 Å, respectively; and it also renders plausible the failure of the isotropic ionic exchange for the X-X interaction. The measured spin-spin interactions are used to calculate the magnetic properties of $La_2Co_3(NO_3)_{12}\cdot 24H_2O$, which are compared with experiment. The susceptibility perpendicular and parallel to the symmetry axis agrees well with the results of Leask and Wolf over the entire temperature range. The calculated magnetic specific-heat tail agrees very well with experimental values reported in the literature. The spin-spin interactions suggest that the ordered state consists of layers of Y ions with their spins along the trigonal axis, and with the layer of X ions on either side ordered in the opposite sense. It is shown that the energy of the antiferromagnetic structure given by alternating the sense of polarization for the X-Y-X sandwiches is only marginally lower than that for the ferrimagnetic array in which all sandwiches are polarized in the same sense. The calculated ordering energy is 6% less than that obtained by Mess *et al.* from calorimetric measurements. The implications of these results for other iron-group ions in the double nitrates and for hydrated complexes in general is briefly examined.

I. INTRODUCTION

THE double nitrate crystals $T_2D_3(NO_3)_{12}\cdot 24H_2O$ provide a veritable magnetic menagerie because of the wide variety of trivalent rare-earth ions that may be substituted for T, and a comparable variety of divalent iron-group ions that may be substituted for D. The spectacular range of magnetic properties is further enhanced by the existence of two types of D sites, the X and Y, with much different crystal fields. The divalent ions are located in hydrated complexes wihch are held together by hydrogen bonding, as is typical of hydrated paramagnetic salts of the iron group. The systematic study of the spin-spin interactions between iron-group ions in the double nitrates could contribute greatly to the general understanding of exchange between ions in hydrated complexes. This paper describes a complete investigation of the spin-spin interactions of Co^{2+} pairs in lanthanum zinc double nitrate (LZN) and in lanthanum magnesium double nitrate (LMN). These results are used to calculate magnetic properties of lanthanum cobalt nitrate (LCN), which are compared with the experimental values to show the relevance of the pair interactions to the concentrated material. Considerable progress is made toward understanding the measured interactions in terms of exchange between orbitals.

The structure of the double nitrates has been given by Zalkin *et al.*[1] The unit cell contains two X ions and one Y ion. The magnetic properties of isolated Co^{2+} ions imply an almost perfectly cubic crystal field in the X site, but a rather large trigonal component for the Y site.[2–4] The divalent ions about an X site are shown in Fig. 1(a), and those about a Y site in Fig. 1(b). The positions and multiplicities of the neighbors are given in Table I. The nearest Y neighbors of a Y site form a hexagon in the basal plane. These sites are 11.0 A away and are not shown in Fig. 1(b). It is found that the dominating interactions are between ions in the nearest-neighbor X sites [$X0$ and $X1$ in Fig. 1(a)], and between ions in the closest pairs of X and Y sites ($X0$ and $Y1$ for example). These interactions are appreciably nondipolar. All other spin-spin interactions are much smaller and are shown to be dipolar to the extent that they can be measured.

An isolated cobalt ion in either site may be described with an effective spin of one-half and the spin

* This work has been supported in part by grants from the National Science Foundation and from the Computation Center of The University of Kansas. A part of this paper is based on the Ph.D. thesis of D. P. Schinke, University of Kansas, 1968 (unpublished). Helium was supplied by the U. S. Office of Naval Research.
† Present address: Bell Telephone Laboratories, Murray Hill, N. J.

[1] A. Zalkin, J. D. Forrester, and D. H. Templeton, J. Chem. Phys. **39**, 2881 (1963).
[2] R. S. Trenam, Proc. Phys. Soc. (London) **A66**, 118 (1953); also thesis, Oxford University, 1953 (unpublished).
[3] J. W. Culvahouse, W. P. Unruh, and D. K. Brice, Phys. Rev. **129**, 2430 (1963).
[4] L. C. Olsen and J. W. Culvahouse, Phys. Rev. **152**, 409 (1966).

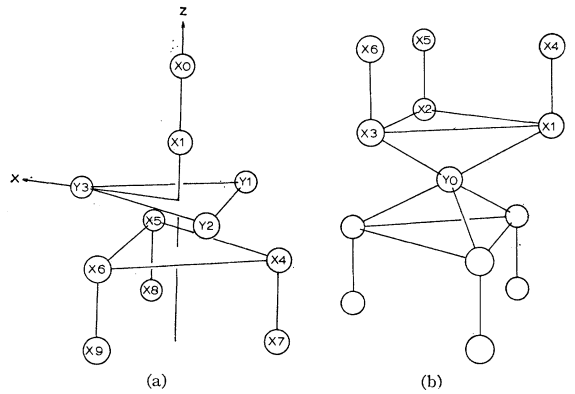

FIG. 1. (a) The divalent neighbors of an X site. (b) The divalent neighbors of a Y site. The scale of distances is given by Table I.

Hamiltonian

$$\mathcal{H}=g_{11}\beta S_z H_z+g_1\beta(H_xS_x+H_yS_y)+AI_zS_z+B(I_xS_x+I_yS_y). \quad (1)$$

The parameters for the ion in the X site exhibit a considerable sensitivity to the divalent constituents. An extensive tabulation of these is given in Table II. The Y ion is far less sensitive to the diamagnetic constituents, and only the values for Co^{2+} in LMN and LZN are given in Table II.

The spin of the 100% abundant Co^{59} is $\frac{7}{2}$ and the spectrum of an isolated ion consists of eight hyperfine lines. The presence of the hyperfine interaction is a complicating feature for the nearest-neighbor X-X pairs since the degeneracy of the product states $S_1{}^z=\pm\frac{1}{2}$ and $S_2{}^z=\mp\frac{1}{2}$ is not removed by the Zeeman interaction. The result is an involved hyperfine structure for the pairs; and for this reason the detailed analysis of the X-X interaction has been given elsewhere[5] as one example of the analysis of the hyperfine structure of pairs of similar ions. For the pairs X-Y, the Zeeman interaction is sufficiently different for the two ions that the transitions of the pairs retain the character of single spin flips, and the hyperfine structure of the pair spectra are replicas of the isolated ion spectrum.

In the next section, the theory for interpreting the experimental data in terms of a phenomenological spin-spin interaction is given. The experimental work is discussed in Sec. III, and the properties of LCN are discussed in Sec. V. Sec. IV contains the interpretation of the nondipolar interaction in terms of superexchange and may be read almost independently of the other sections.

TABLE I. Divalent neighbors of X and Y ions. The coordinate ρ_1 is measured in the plane perpendicular to the symmetry axis, and z is along the symmetry axis. The distances are in Angstrom units. The last column is the dipolar contribution to J_{00}.

Order of nearness	Number	Type	ρ_1	z	r	$J_{00}{}^{(d)}/2g\beta$ (G)
			X Ion			
1	1	X	0.00	4.99	4.99	−327
2	3	Y	6.35	3.27	7.14	+34.7
3	3	X	6.35	6.54	9.12	−13.0
4	3	Y	6.35	8.22	10.39	−26.7
5	6	X	11.00	0.00	11.00	+15.2
			Y Ion			
1	6	X	6.35	±3.35	7.14	+20.6
2	6	X	6.35	±8.22	10.39	−15.9
3	6	Y	11.00	0.00	11.00	+25.6

[5] J. W. Culvahouse, D. P. Schinke, and L. G. Pfortmiller, Phys. Rev. **177**, 454 (1969).

II. THEORETICAL PRELIMINARIES

The general bilinear form of the spin-spin interaction may be written in terms of spherical tensor operators[6] as

$$\mathcal{H}_{12}=\sum_{qq'}\mathcal{J}_{qq'}(1,2)T_{1q}(S_1)T_{1q'}(S_2), \quad (2)$$

where

$$T_{10}=S_z, \quad T_{1\pm1}=\mp S_\pm/\sqrt{2}, \quad (3)$$

and the rule for forming the Hermitian adjoint is

$$(T_{iq})^\dagger=(-1)^qT_{1-q}. \quad (4)$$

The constants $\mathcal{J}_{qq'}(1,2)$ are complex, but the Hermiticity requirement and (4) imply

$$\mathcal{J}_{qq'}{}^*=(-1)^{q+q'}\mathcal{J}_{-q-q'}, \quad (5)$$

and

$$\mathcal{J}_{00}=J_{00}, \quad (6)$$

where J_{00} is real. The argument of $\mathcal{J}_{qq'}$ has been omitted in (5) and (6) and is to be assumed (1,2) here and elsewhere. These relations reduce the total number of constants to nine. If there is an inversion center between the two ions, the interaction must be symmetric in the interchange of the two spin operators and the number of constants is reduced to six by the requirement

$$\mathcal{J}_{qq'}=\mathcal{J}_{q'q}, \quad (7)$$

which is equivalent to starting that the Moriya-Dzyaloshinski form[7]

$$\mathbf{D}\cdot(\mathbf{S}_1\times\mathbf{S}_2) \quad (8)$$

is not present. The angular dependence of the spin-spin effects emerges most naturally if phase factors are used to describe the complex character of $\mathcal{J}_{qq'}$. We write

$$\mathcal{J}_{qq'}=J_{qq'}e^{i\phi_{qq'}}, \quad (9)$$

and the Hermiticity requirement implies

$$\phi_{00}=0, \quad \phi_{-q-q'}=-\phi_{-q-q'}, \quad (10)$$

and

$$J_{qq'}=(-1)^{q+q'}J_{-q-q'}. \quad (11)$$

[6] A. R. Edmonds, *Angular Momentum in Quantum Mechanics* (Princeton University Press, Princeton, N. J., 1957).

[7] I. Dzyaloshinski, Phys. Chem. Solids **4**, 241 (1958); T. Moriya, Phys. Rev. **117**, 635 (1960).

TABLE II. Spin-Hamiltonian parameters for Co^{2+} in a number of double nitrates. The spin contribution to g is given in the last two columns.

Material	$g_{\parallel}$	$g_{\perp}$	$g_{\parallel}+2g_{\perp}$	A (10^{-4} cm^{-1})	B (10^{-4} cm^{-1})	$g_{s\parallel}$	$g_{s\perp}$
			X Ion				
LMN[a]	4.057±0.003	4.445±0.003	12.945	78.4±0.5	104.3±0.5	3.17	3.40
LZN[f]	4.37 ±0.01	4.31 ±0.01	12.99	98.9±0.5	94.8±0.5	3.35	3.32
BiMN[c]	4.108±0.003	4.385±0.003	12.88	85.0±1.0	103.0±1.0	3.20	3.36
CeZN[b]	4.37 ±0.03	4.31 ±0.03	13.0	99.0±2.0	95.0±2.0	3.35	3.32
LZN[d] (D_{2b})	4.50 ±0.01	4.22 ±0.01	12.94	107.6±1.0	89.7±1.0	3.43	3.27
NdZN[e]	4.38 ±0.02	4.28 ±0.03	12.98	100.0±2.0	93.0±2.0	3.36	3.31
LMN[f] (*X-Xpr*)	4.31 ±0.02	4.32 ±0.02	12.95	95.5±1.0	99.5±3.0	3.33	3.33
			Y Ion				
LZN[b]	7.36 ±0.01	2.337±0.005	12.04	292.0±1.0	3	5.18	1.99
LMN[c]	7.35 ±0.01	2.325±0.003	12.00	286.6±1.4	3	5.18	1.99

[a] W. P. Unruh, Ph.D. thesis, The University of Kansas, 1962 (unpublished).
[b] Reference 10, but note that the values given for CZN are revised values reported by F. Carboni and R. C. Sapp, Ann. Phys. (N. Y.), 1, 77 (1965).
[c] Reference 2. The LMN data is reported only in the thesis.
[d] Reference 3.
[e] Reference 11.
[f] Reference 5.

We assume in our discussion that the Zeeman interaction is the dominant term in the Hamiltonian

$$\mathcal{H}=\mathcal{H}_1+\mathcal{H}_2+\mathcal{H}_{12} \tag{12}$$

for a pair of ions. If $\mathcal{H}_1$ and $\mathcal{H}_2$ are characterized by trigonal or higher symmetry, the g tensor is axially symmetric and the Zeeman interaction can be made diagonal for a field at the angle θ with the symmetry axis by selecting a quantization axis for the spin i which is at angle β_i from the trigonal axis; and β_i is given by[8]

$$\tan\beta_i=[g_{\perp}(i)/g_{\parallel}(i)]\tan\theta \tag{13}$$

and the Zeeman energy is given by

$$\mathcal{H}_z(i)=g_i\beta HS_z, \tag{14}$$

where

$$g_i=\{[g_{\parallel}(i)]^2[\cos\theta]^2+[g_{\perp}(i)]^2[\sin\theta]^2\}^{1/2}. \tag{15}$$

If the two ions have different g tensors, the quantization axes are different for the two ions and the operators for spin number one and spin number two must be quantized along different axes z_1' and z_2' at angles β_1 and β_2 with the symmetry axis. The best direction for the quantization of the nuclear spin is the direction $(\mathbf{g}_i\cdot\mathbf{H})\cdot\mathbf{A}_i$, but this aspect of the problem will not enter our discussion in an important way. The perturbative treatment is facilitated by transforming the tensor operators in (2) to sets of axes with the z axis in the direction z_1' and z_2' for the two spin operators. This is accomplished by rotations defined by the Euler angles[9] $(\alpha_1,\beta_1,0)$ and $(\alpha_2,\beta_2,0)$, where the third Euler angle has been taken to be zero because it corresponds to a rotation about the quantization axis and merely introduces an unimportant phase factor. We will assume that the tensor operators and their coefficients in (2) are referred to a common set of crystal axes for which the symmetry axis is the z axis. The first Euler angle will then be the same for the two ions and will be the angle ϕ between the plane defined by the magnetic field and the trigonal axis and the x-z plane of the crystal axes. To avoid a cumbersome notation, we shall designate the spin-spin interaction constant and tensor operators referred to these new axes with a prime. The prime will not be used for the effective g and A values. Thus

$$T_{1q}'(S_1)=\sum_{q'}T_{1q'}D_{q'q}^{(1)}(\phi,\beta_1,0) \tag{16a}$$

and

$$T_{1q}'(S_2)=\sum_{q'}T_{1q'}D_{q'q}^{(1)}(\phi,\beta_2,0), \tag{16b}$$

where the rotation matrices $D_{mm'}^{(l)}$ are those defined by Tinkham and others.[9] The coefficients of the primed operators are given by the transformation rule

$$\mathcal{J}_{q_1q_2'}=\sum_{q_1'q_2'}\mathcal{J}_{q_1'q_2'}[D_{q_1q_1'}^{(1)}(0,-\beta_1,-\phi)\times D_{q_2q_2'}^{(1)}(0,-\beta_2,-\phi)], \tag{17}$$

which is implied by the invariance of the Hamiltonian under a rotation of the coordinate axes. The complete Hamiltonian assumes the form

$$\mathcal{H}=g_1\beta HS_1^{z'}+g_2\beta HS_2^{z'}+A_1I_1^{z'}S_1^{z'}+A_2I_2^{z'}S_2^{z'}+\sum_{qq'}\mathcal{J}_{qq'}T_{1q}'(S_1)T_{1q'}'(S_2)+\text{off-diagonal hyperfine terms}, \tag{18}$$

and the diagonal elements in a product representation are

$$\langle+,+|\mathcal{H}|+,+\rangle=\tfrac{1}{2}(g_1+g_2)\beta H+\tfrac{1}{2}(A_1m_1+A_2m_2)+\tfrac{1}{4}J_{00}', \tag{19a}$$

$$\langle+,-|\mathcal{H}|+,-\rangle=\tfrac{1}{2}(g_1-g_2)\beta H+\tfrac{1}{2}(A_1m_1-A_2m_2)-\tfrac{1}{4}J_{00}', \tag{19b}$$

[8] B. Bleaney, Phil. Mag. 42, 441 (1951).
[9] M. Tinkham, *Group Theory and Quantum Mechanics* (McGraw-Hill Book Co., New York, 1964), p. 111.

$$\langle -,+|\mathcal{H}|-,+\rangle=\tfrac{1}{2}(g_2-g_1)\beta H +\tfrac{1}{2}(A_2m_2-A_1m_1)-\tfrac{1}{4}J_{00}', \quad (19c)$$

and

$$\langle -,-|\mathcal{H}|-,-\rangle=-\tfrac{1}{2}(g_1+g_2)\beta H -\tfrac{1}{2}(A_1m_1+A_2m_2)+\tfrac{1}{4}J_{00}', \quad (19d)$$

where

$$A_i=(1/g_i)\{A^2[g_{11}(i)]^2[\cos\theta]^2 +B^2[g_1(i)]^2[\sin\theta]^2\}^{1/2} \quad (20)$$

and m_1, m_2 are the quantum numbers for the projection of the nuclear spin on the directions $(\mathbf{g}_1\cdot\mathbf{H})\cdot\mathbf{A}_1$ and $(\mathbf{g}_2\cdot\mathbf{H})\cdot\mathbf{A}_2$.

The suitability of the product representation for the calculation of the energy eigenvalues depends upon the Zeeman energies $g_1\beta H$, $g_2\beta H$, and $(g_1-g_2)\beta H$ being much larger than the off-diagonal matrix elements of the spin-spin and hyperfine interactions. For similar ions such as the X-X pairs, the levels $|+,-,m_1m_2\rangle$ and $|-,+,m_1m_2\rangle$ are degenerate in this order of perturbation theory and it is more useful to begin the calculation in the singlet-triplet representation for the two ionic spins (see Ref. 5). For the spin-spin interactions analyzed in the next section, adequate observations can be made for field directions such that $(g_1-g_2)\beta H$ is much greater than the spin-spin and the hyperfine interaction coefficients. Quite accurate results are then given by Eqs. (19). Those transitions corresponding to a change in the z component of spin one are at magnetic fields

$$H^{(1)}(m_1)=H_1+\frac{A_1m_1}{2g_1\beta}+\frac{J_{00}'}{2g_1\beta} \quad (21a)$$

and

$$H^{(2)}(m_1)=H_1+\frac{A_1m_1}{2g_1\beta}-\frac{J_{00}'}{2g_1\beta}, \quad (21b)$$

where $H_1=h\nu/g_1\beta$ and ν is the observing frequency. The sets of transitions (21a) and (21b) form an exact replica of the spectrum of an isolated ion of type one shifted up and down in field by $J_{00}'/g_1\beta$. There are two other sets of pair transitions corresponding to transitions in which the z component of spin two changes. These are exact replicas of the spectrum of ioslated ions of type two and are shifted up and down in field by $J_{00}'/g_2\beta$ relative to that of the isolated ions.

The sign of J_{00}' can be determined from the temperature dependence of the relative intensity of the high-field and low-field pairs about an isolated ion spectrum. The intensity of the high-field pairs relative to the low-field pairs is given by $\exp\{(h\nu/kT)(J_{00}'/|J_{00}'|)\}$.

The second-order effects of the spin-spin interaction produce the same displacement for the high-field and low-field pairs so that the centroid of the pair spectra is shifted relative to that of the isolated ion spectrum by

$$\delta H_1^{(2\text{nd})}=-\left(\frac{1}{g_1\beta}\right)\left(\frac{1}{4h\nu}\right)\left[(J_{10}')^2+\left(\frac{g_1}{g_1-g_2}\right)(J_{1-1}')^2 +\left(\frac{g_1}{g_1+g_2}\right)(J_{11}')^2\right], \quad (22)$$

where only the Zeeman interaction has been used to determine the energy eigenvalues and the field has been assumed to be $H_1=h\nu/g_1\beta$. Therefore, among the third order corrections, there are terms which arise from the diagonal matrix elements of the spin-spin and hyperfine interactions. Equation (22) can give a positive value for the shift if $g_2>g_1$. The corresponding centroid shift for the pair spectra about the spectrum of the isolated ions of type two is of interest because it involves J_{01}' rather than J_{10}'. For it we find

$$\delta H_2^{(2\text{nd})}=-\left(\frac{1}{g_2\beta}\right)\left(\frac{1}{4h\nu}\right)\left[(J_{01}')^2+\left(\frac{g_2}{g_2-g_1}\right)(J_{1-1}')^2 +\left(\frac{g_2}{g_1+g_2}\right)(J_{11}')^2\right]. \quad (23)$$

To the third order in perturbation theory, the separation of the high- and low-field pair spectra about isolated ion resonances of ions one and two are given by

$$\Delta H_1=J_{00}'/g_1\beta \quad (24a)$$

and

$$\Delta H_2'=J_{00}'/g_2\beta. \quad (24b)$$

An additional shift of the centroid of the pair spectra relative to that of the isolated ion may be produced by a change in the g tensor of an ion which is a member of the pair. The first-order effect of the change in the g tensor is given by the change in the effective g value, which we designate δg. The shift of the centroid in magnetic fields units is $-(\delta g/g)(h\nu/g\beta)$. The total centroid shift for the pair spectra about that of isolated ions of type one is

$$\delta H_1=\delta H_1^{(2\text{nd})}-\left(\frac{\delta g_1}{g_1}\right)\left(\frac{h\nu}{g_1\beta}\right) =\left(\frac{M_1}{g_1\beta}\right)\left(\frac{1}{h\nu}\right)-\left(\frac{\delta g_1}{g_1^2\beta}\right)(h\nu), \quad (25)$$

where

$$M_1=\delta H_1^{(2\text{nd})}g_1\beta h\nu,$$

and the second form of (25) emphasizes the fact that the magnitude of the second-order shifts is inversely proportional to the frequency and the g-factor shifts are proportional to the frequency, so that measurements at two frequencies are adequate to determine each effect separately.

In cases where the perturbation treatment is accurate, the spin-spin interaction coefficients corresponding to the part of $\mathcal{H}_{12}$ that is symmetric under the interchange of the two spins can be determined from the angular dependence of J_{00}', which from (17) is given by

$$\begin{aligned} J_{00}' = J_{00}\cos\beta_1\cos\beta_2 - \sqrt{2}J_{10}\cos(\phi+\phi_{10})\sin\beta_1\cos\beta_2 \\ -\sqrt{2}J_{01}\cos(\phi+\phi_{01})\sin\beta_2\cos\beta_1 \\ -J_{1-1}\cos\phi_{1-1}\sin\beta_1\sin\beta_2 \\ +J_{11}\cos(2\phi+\phi_{11})\sin\beta_1\sin\beta_2. \end{aligned} \quad (26)$$

From (24) and (26), we see that J_{00} is determined by the separation of the pair spectra with the field along the symmetry axis. Three more constants ($J_{1-1}\cos\phi_{1-1}$, J_{11}, and ϕ_{11}) can be determined from the values of J_{00}' for the magnetic field in the plane perpendicular to the symmetry axis for which (26) reduces to

$$J_{00}(90°,\phi) = -J_{1-1}\cos\phi_{1-1} + J_{11}\cos(2\phi+\phi_{11}). \quad (27)$$

Two more constants can be determined from the terms in (26) which are linear in $\sin\beta_1$ and $\sin\beta_2$. The form of (26) suggests that the phase and amplitude of the coefficients of each of the two terms can be determined separately, but from (13) the angular factors are linearly dependent:

$$\sin\beta_2\cos\beta_1 = a\sin\beta_1\cos\beta_2, \quad (28)$$

where

$$a = [g_\perp(2)g_{11}(1)]/[g_\perp(1)g_{11}(2)]. \quad (29)$$

The terms may be rewritten as

$$R = \sin\beta_1\cos\beta_2\bar{J}_{10}\cos(\phi+\bar{\phi}), \quad (30)$$

where

$$\bar{J}_{10} = [(J_{10})^2 + a^2(J_{01})^2 + 2aJ_{10}J_{01}\cos(\phi_{10}-\phi_{01})]^{1/2} \quad (31)$$

and

$$\cos\bar{\phi} = [J_{10}\cos\phi_{10} + aJ_{01}\cos\phi_{01}/J_{10}]. \quad (32)$$

The value of $\bar{J}_{10}$ and $\bar{\phi}$ can be determined quite easily from measurements with the magnetic field at small angles θ with the symmetry axis because the contribution which depends on those values is distinguished by a linear dependence for small values of θ and particularly by a change in sign as the field is varied through the direction of the symmetry axis (because ϕ changes by π). The determination of these two constants is equivalent to measuring $\mathcal{J}_{10}+\mathcal{J}_{01}$.

Altogether, six constraints on the nine constants are given by the measurement of ΔH for different field directions. These constraints determine the spin-spin interaction completely if it is known to be symmetric in the interchange of the two spins. Further information cannot be obtained from J_{00}' because it is symmetric in the interchange of the spins (β_1 and β_2 will be interchanged as well as the subscripts on the spin-spin coefficients).

For information on the antisymmetric part of the interaction one must turn to the second-order shifts given by (22) and (23), for only these involve terms which are not symmetric for the interchange of the two spins. For the magnetic field in the direction defined by the spherical coordinates θ and ϕ, we have from (17)

$$\begin{aligned} \mathcal{J}_{10}' = \tfrac{1}{2}\{2J_{10}\cos(\phi+\phi_{10})\cos\beta_1\cos\beta_2 + \sqrt{2}J_{00}\sin\beta_1\cos\beta_2 \\ +\sqrt{2}[J_{1-1}\cos\phi_{1-1} - J_{11}\cos(2\phi+\phi_{11})]\cos\beta_1\sin\beta_2\} \\ +(\tfrac{1}{2}i)\{2J_{10}\sin(\phi+\phi_{10})\cos\beta_2 \\ +\sqrt{2}[J_{1-1}\sin\phi_{1-1} - J_{11}\sin(2\phi+\phi_{11})]\sin\beta_2 \\ -2iJ_{01}\sin(\phi+\phi_{01})\sin\beta_1\sin\beta_2\}, \end{aligned} \quad (33)$$

$$\begin{aligned} \mathcal{J}_{1-1}' = -\tfrac{1}{2}\{J_{00}\sin\beta_1\sin\beta_2 + \sqrt{2}J_{10}\cos(\phi+\phi_{10})\cos\beta_1\sin\beta_2 \\ +\sqrt{2}J_{01}\cos(\phi+\phi_{01})\sin\beta_1\cos\beta_2 - J_{11}\cos(2\phi+\phi_{11}) \\ \times(1-\cos\beta_1\cos\beta_2) - J_{1-1}\cos\phi_{1-1}(1+\cos\beta_1\cos\beta_2)\} \\ -(\tfrac{1}{2}i)\{\sqrt{2}J_{10}\sin(\phi+\phi_{10})\sin\beta_2 - \sqrt{2}J_{01}\sin(\phi+\phi_{01})\sin\beta_1 \\ -J_{11}\sin(2\phi+\phi_{11})(\cos\beta_1-\cos\beta_2) \\ -J_{1-1}\sin\phi_{1-1}(\cos\beta_1+\cos\beta_2)\}, \end{aligned} \quad (34)$$

and

$$\begin{aligned} \mathcal{J}_{11}' = \tfrac{1}{2}\{J_{00}\sin\beta_1\sin\beta_2 + \sqrt{2}J_{10}\cos(\phi+\phi_{10})\cos\beta_1\sin\beta_2 \\ +\sqrt{2}J_{01}\cos(\phi+\phi_{01})\sin\beta_1\cos\beta_2 + J_{11}\cos(2\phi+\phi_{11}) \\ \times(1+\cos\beta_1\cos\beta_2) + J_{1-1}\cos\phi_{1-1}(1-\cos\beta_1\cos\beta_2)\} \\ +(\tfrac{1}{2}i)\{\sqrt{2}J_{10}\sin(\phi+\phi_{10})\sin\beta_2 + \sqrt{2}J_{01}\sin(\phi+\phi_{01})\sin\beta_1 \\ +J_{11}\sin(2\phi+\phi_{11})(\cos\beta_1+\cos\beta_2) \\ +J_{1-1}\sin\phi_{1-1}(\cos\beta_1-\cos\beta_2)\}. \end{aligned} \quad (35)$$

The determination of the antisymmetric terms from the second-order shifts is feasible in general only if they are at least comparable with the other terms in the spin-spin interaction. It is only after the maximum number of constants have been determined from measurements of ΔH that one can analyze (33)–(35) to determine the directions of maximum sensitivity to the antisymmetric terms. Even then, the determination of directions of maximum sensitivity is in general a formidable numerical investigation. If the antisymmetric terms are large and therefore important in determining the magnetic and thermal properties of the concentrated system, the second-order shifts will yield their values rather directly.

III. EXPERIMENTAL RESULTS

The measurements reported here were made with a superheterodyne spectrometer operating between 12.8 and 17 GHz; and a 36–39 GHz spectrometer with a microwave biased balanced mixer and 8-KHz magnetic field modulation. The magnetic field measurements were made with a Varian Mark I Field Dial calibrated to an accuracy of about 2 G. All of the measurements were made at 4.2°K unless explicitly stated otherwise. Except in those cases where the exact frequency is important, the frequency will be designated as 16 and 37 GHz to distinguish the two ranges. The concentration of Co^{2+} in most cases was 1% of the divalent ions.

The cobalt pair spectra have been studied in LMN and LZN, and the results for the two nearest pairs are

TABLE III. The measured spin-spin interaction constants of X-Y pairs in LZN and LMN in units of cm^{-1}. The calculated dipolar contributions are also tabulated and the last entry labeled "Residual" is the difference of the measured and dipolar values, assuming the most favorable choice of phase angles ϕ_{ij} allowed by the ambiguities discussed in the text.

	Lanthanum zinc nitrate			Lanthanum magnesium nitrate		
	Measured	Dipolar	Residual	Measured	Dipolar	Residual
J_{00}	0.2040±0.0020	0.0141	0.1899±0.0020	0.1925±0.0015	0.0131	0.1794±0.0015
J_{1-1}	−0.0752±0.0015	0.0022	−0.0774±0.0015	−0.0715±0.0014	0.0023	−0.0738±0.0014
J_{11}	−0.0171±0.0020	−0.0142	−0.0029±0.0020	−0.0166±0.0020	−0.0146	−0.0020±0.0020
J_{10}	<0.06	0.0324	···	<0.06	0.0334	···
J_{01}	<0.03	0.0105	···	<0.03	0.0097	···
$\bar{J}_{10}$	0.0340±0.0015	0.0358	−0.0018±0.0015	0.0361±0.0018	0.0363	−0.0002±0.0018
ϕ_{1-1}	<35°	0°	···	<35°	0°	···
ϕ_{11}	0°±4°	0°	···	0°±4°	0°	···
ϕ_{01}	···	0°	···	···	0°	···
ϕ_{10}	···	0°	···	···	0°	···
$\bar{\phi}$	0°±8°	0°	···	0°±8°	0°	···

tabulated in Table III for both crystals. The spin-spin interactions are very similar, and the major difference in the appearance of the spectra arises from the fact that the g factor of the X-X pairs is virtually identical to that of isolated ions in LZN for both crystals, with the result that there is a considerable g shift of the X-X spectra relative to the isolated X ion spectrum in LMN. This feature was an aid in the study of the X-X pairs, and the results presented in Ref. 5 were based entirely on spectra taken with LMN. In this section which is devoted primarily to the X-Y pairs, most of the examples are for LZN.

A. Spin-Spin Interaction X-Y

Figure 2 illustrates the general pattern of the isolated ion resonances and the most prominent pairs for Co^{2+} in LMN for the magnetic field along the symmetry axis and an observing frequency of about 16 HGz. Each block represents the hyperfine structure, a simple eight line spectrum except for the X-X pairs. The spectrum of LMN was chosen for this example because the large g shift of the X-X pairs permits one to see more of the X-X spectrum. Much better separation of all pairs is obtained at 37 GHz. In the discussion of these spectra, we shall refer to the spectrum of an isolated X ion or Y ion as simply the X or Y spectrum, the spectra

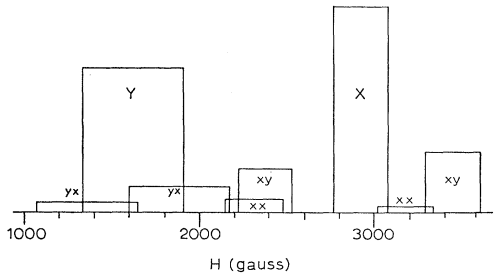

FIG. 2. A schematic representation of the EPR spectrum of Co^{2+} in LMN at 16 GHz with the magnetic field along the symmetry axis. Each block represents the hyperfine structure. The spectrum X-X is shifted to lower field becausee the value of g_{II} is higher than for isolated X ions. Better separations are obtained at 37 GHz.

of X-Y pairs about the isolated X ion resonance as the X-Y spectra, and the spectra of X-Y pairs about the isolated Y-ion spectrum as the Y-X spectra. It is to be understood that the X-Y pairs are the nearest such pairs unless stated otherwise. In using the nomenclature of Sec. II, we shall consider the X ion to be the ion of type 1, and understand the argument of $\mathcal{J}_{qq}$ to be (X,Y), although the order is significant only for the antisymmetric parts of the interaction.

For the magnetic field perpendicular to the symmetry axis, the Y spectrum is highest ($g_1 \sim 2.3$), the X spectrum ($g_1 \sim 4.3$) is lowest; there is a good separation of the X-Y and Y-X spectra, even at 16 GHz. This field direction gives a particularly clear view of the Y-X spectrum at 37 GHz. For the Y ion $B \sim 0$, and the hyperfine structure is determined by second-order effects of A, which give rise to four unequally spaced lines. At 16 GHz this second-order effect is large enough that the individual spectra are difficult to analyze with precision. At 37 GHz, the total spread of the structure is only 15 G, so that one has a single line hardly any broader than the individual hyperfine lines.

As the field direction is varied away from the direction of the symmetry axis, the X and Y spectra approach each other. This results in an overlap of the X-Y and Y-X spectra and rapidly increasing second-order effects. Useful data can be obtained only within 25° of the symmetry axis at 16 GHz and within 30° at 37 GHz. Data taken with the field a few degrees out of the plane perpendicular to the symmetry axis are not useful because of the complicated overlapping patterns about the X-spectrum and because of the rapid broadening of the Y ion spectrum by a diagonal contribution to the hyperfine structure. Thus our data are limited to field directions in the range about the symmetry axis defined above and to directions in the plane perpendicular to the symmetry axis.

The identifications of the spectra indicated in Fig. 2 were made as follows: First it was verified that the intensity of the pair spectra relative to that of the isolated ions varied in proportion to the concentration in the range 0.5–3%. The identification of the X-X

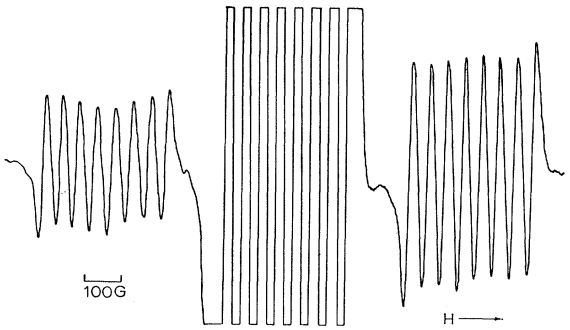

FIG. 3. The X-Y spectrum of LZN with the magnetic field along the symmetry axis for a frequency of 37 GHz. As explained in the text, this is the spectrum of an X ion with a Y ion neighbor with the spectrum of the isolated X ion in the center.

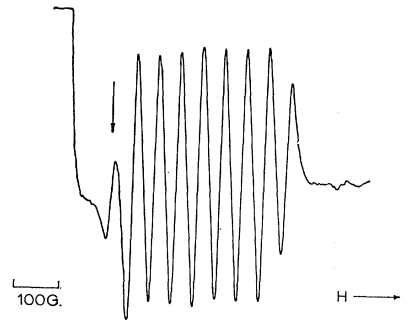

FIG. 4. The X-Y spectrum of LZN at 37 GHZ with the magnetic field 13° from the symmetry axis and in the plane defined by $\phi=0$. The spectrum has separated into two parts or relative intensities one and two, which correspond to the two different values of $\cos\phi$ for the pairs. The separation of these components provide the data for Figs. 7 and 8.

spectrum was made from the observation that it shows a complicated hyperfine pattern that can be explained both for the field along and perpendicular to the symmetry axis by assuming an axial spin-spin interaction between two X ions. Furthermore, the X-X spectrum is invariant as the field direction is varied in the plane perpendicular to the symmetry axis as expected for an interionic axis along the symmetry axis (for details, see Ref. 5). The salient features for the identification of the X-Y and Y-X spectra are pointed out below in the discussion of the spectra.

The derivative of absorption for the high- and low-field X-Y components are shown in Fig. 3 for $\nu=37.63$ GHz, the field along the symmetry axis, and a LZN crystal. That this spectrum is not due to axial pairs is shown immediately by one taken with H slightly off the symmetry axis, as shown in Fig. 4. For this spectrum $\theta=13°$, and $\mathbf{H}$ is in a plane $\phi=0$ defined by the trigonal axis and the bisector of one of the sides of the hexagonal plates in which the double nitrates crystallize. The pair spectrum in Fig. 4 consists of two sets of hyperfine lines of relative intensity 2:1 and shifted by one hyperfine interval relative to each other. This behavior is completely consistent with the prediction of Eq. (26) for a set of either three or six pairs, one-third with $\cos\phi=1$ and two thirds with $\cos\phi=-\frac{1}{2}$. For other values of ϕ, the spectrum splits into three sets of equal intensity. That these are X-Y pairs rather than X-X pairs is strongly suggested by the fact that the hyperfine structure is a simple replica of the X spectrum. Such a simple pattern could arise from an X-X pair only if $J_{1-1}'\ll A$, which could be true for one direction of the field, but not for both of the directions represented by Figs. 3 and 4. Further evidence that these are X-Y pair spectra—perhaps more compelling—is the relationship of the pair spectra labeled X-Y and Y-X in Fig. 2. For the field along the symmetry axis, the separation of the high- and low-field pairs about the X and Y spectra as determined from spectra taken at 37 GHz is precisely in the ratio $g_{11}(Y)/g_{11}(X)$, as is predicted by Eqs. (24). Small deviations from this ratio in spectra taken at 16 GHz can be ascribed to third-order effects on the Y-X pairs. This relationship between the X-Y and Y-X has been verified for many other field directions.

As shown in the last section, there are nine constants to be determined for an X-Y interaction, and six can be extracted from measurements of ΔH. J_{00} is given directly by the spectrum shown in Fig. 3, and equivalent ones taken at both 37 and 16 GHz are the source of the values tabulated for this quantity in Table III. The sign is that implied by intensity measurements described below.

The angular variation of J_{00}' in the plane perpendicular to the symmetry axis and the fit of the results to Eq. (27) determines J_{1-1}, J_{11}, and ϕ_{11}. For this series of measurements, the Y-X spectra at 37 GHz provide the most accurate results. An example is given in Fig. 5 for which $\phi=34°$. As explained at the beginning of this section, the hyperfine splitting is negligible here. There are two resolved lines on the high-field side, and the line nearest the Y spectrum is twice as intense as the outer one. This is in accord with Eq. (27) if there are three or six ions, two-thirds with $\cos(2\phi+\phi_{11})=\pm\frac{1}{2}$ and one-third with $\cos(2\phi+\phi_{11})=\pm1$. For the low-field lines, the two interior lines do not quite conincide. This difference in the angles for which the high- and low-field

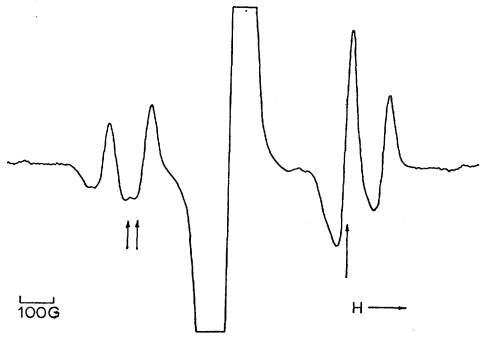

FIG. 5. The spectrum Y-X of LZN at 37 GHz and the magnetic field perpendicular to the symmetry axis and in the plane $\phi=34°$. The inner two lines of the low-field spectrum merge at $\phi=26°$, the result of a ϱ shift.

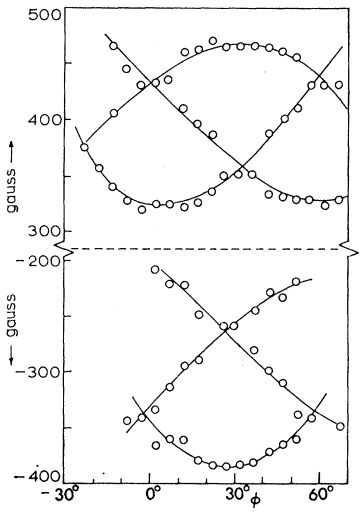

FIG. 6. The angular variation of the components of the Y-X spectrum of LZN at 37 GHz and the magnetic field in the basal plane. J_{11}, $J_{1-1}\cos\phi_{1-1}$, and ϕ_{11} are determined from this data.

lines merge is shown quite clearly in Fig. 6, which is a plot of the line positions as a function of the angle ϕ. This difference arises from a ϕ-dependent g shift discussed in Appendix A. If the separation ΔH of the high- and low-field lines is plotted as a function of ϕ, it is found that the maximum separation occurs for $\phi=30°$ (modulo 60) within the experimental error of about 4°. This data implies that $\phi_{11}=-60°$ (modulo 120) if J_{11} and $J_{1-1}\cos\phi_{1-1}$ are taken to have the opposite sign. If the same signs are given to J_{11} and $J_{1-1}\cos\phi_{1-1}$, then $\phi_{11}=0°$ (modulo 120°). The 60° ambiguity in ϕ and the corresponding 120° ambiguity in ϕ_{11} are fundamental since there is no way to know which of the neighbors is associated with a particular line.

As suggested in Sec. II, the angular dependence of ΔH near $\theta=0°$ provides the most direct measure of $\bar{J}_{10}$ and $\bar{\phi}$. In one analysis, ΔH was measured as a function of θ for the range 30° either side of the symmetry axis; the contribution of J_{00}, J_{11}, and J_{1-1} was subtracted thus forming the quantity R defined by Eq. (30). The results for the plane defined by $\phi=0$ are given in Fig. 7. The open circles and plus signs represent the position of the lines which remain degenerate and correspond to $\phi+\bar{\phi}=\pm 120°$. The crosses correspond to the lines which are half as intense as the degenerate pair and correspond to the ions for which $\phi+\bar{\phi}=0°$. The data has been taken from measurements at both 37 and 16 GHz. The slopes of the two sets are indeed of the opposite sign and twice as large for one as for the other, in agreement with Eq. (30). The scatter of the data arises primarily from the difficulty of measuring the separation of the overlapping hyperfine structures, as may be judged from Figs. 3 and 4. At the larger angles higher-order perturbations and strain-induced changes in the g tensor are beginning to have appreciable effects. The data are fitted by Eq. (30) with a standard deviation of only 7 G, yielding $\bar{J}_{10}/g_1\beta=168$ G. In another analysis, the angles for which the two sets of lines are shifted by $A/2$, A, and $3A/2$ relative to each other were used to determine J_{10} with similar results.

The variation of R with ϕ is shown in Fig. 8. This gives $\bar{\phi}=0°$ (modulo 60°). The periodicity of the pattern is actually 120°, but the orientation of the crystal by the external faces is defined only within a multiple of 60°. The result is equivalent to an ambiguity in the sign of $\bar{J}_{10}$ relative to J_{00} that could be removed by x-ray orientation of the crystal.

These examples show how the six constants J_{00}, $J_{1-1}\cos\phi_{1-1}$, J_{11}, ϕ_{11}, $\bar{J}_{10}$, and $\bar{\phi}$ can be obtained from the measurement of the separation of the high- and low-field pairs. Except for the residual ambiguity in the values of ϕ_{11} and $\bar{\phi}$, only the signs of J_{00} and $J_{1-1}\cos\phi_{1-1}$ are required to complete the determination of the symmetric part of the X-Y interaction. These signs are determined by the temperature dependence of the relative intensity of the high- and low-field pairs with the magnetic field along the symmetry axis and perpendicular to it. The results for a set of such measurements on the X-Y spectrum with the magnetic field along the symmetry axis are given in Fig. 9. The dashed curves are the theoretical variations for the two signs of J_{00}. Clearly J_{00} is positive. With the magnetic field perpendicular to the symmetry axis the high-field lines of the Y-X spectrum become strong relative to the low-field lines as the temperature is lowered. This result implies that $J_{1-1}\cos\phi_{1-1}$ is negative. These are the signs which correspond to an antiferromagnetic interaction; they can be anticipated from Figs. 3 and 4, which show the high-field lines stronger even at 4.2°K.

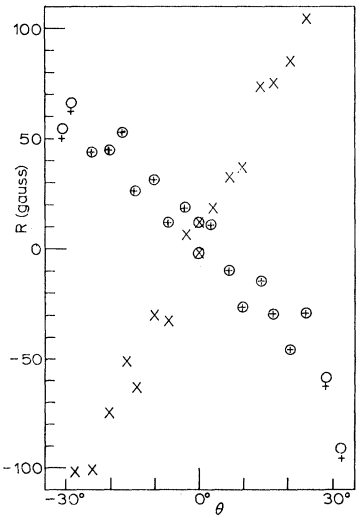

FIG. 7. A plot of the experimental results for R as defined by Eq. (30) for X-Y of LZN. Data taken at 16 and 37 GHz are represented in the plot. The crosses are the results for the lines of intensity one, and the circles and plus signs for the lines that are degenerate at small θ. At the larger angles, these lines separate slightly because of imperfect alignment.

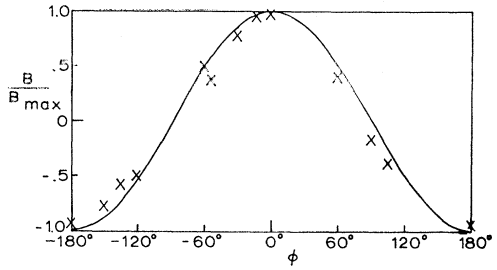

FIG. 8. The variation of R for LZN at 16 GHz as the angle ϕ is varied. The field directions were on a cone opening 15° from the symmetry axis.

The data presented in this section illustrate the results which were most sensitive to the symmetric part of the X-Y interaction. The results presented in Table III are the best values based on the analysis of many experiments on crystals ranging in concentration from 0.5–3%, at both frequencies and on the X-Y as well as the Y-X spectra. The phase angles listed in Table III are modulo 120°. There is a sign uncertainty in $\tilde{J}_{10}$ which is equivalent to the 60° ambiguity in ϕ mentioned above.

B. Centroid Shifts

If ϕ_{1-1} and the two parameters corresponding to $(\mathcal{J}_{10}-\mathcal{J}_{01})$ are to be determined, it must be done from the second-order effects as they are reflected in the centroid shifts. Despite the difficulty in analyzing Eqs. (33)–(35), the large magnitude of J_{00} makes it quite apparent that the symmetry axis is the direction offering maximum sensitivity to these antisymmetric components.

Measurements of the X-Y spectrum of LZN with the field along the symmetry axis give centroid shifts of 4.5±3.0 and 14.0±2.0 G at 37 and 16 GHz. Analysis of these results with Eq. (25) yields

$$\delta H_1^{(2\mathrm{nd})} = 14.7 \pm 4.0 \text{ G (at 16 GHz)}$$

and

$$\delta g_{zz}(X) = f_{zz}(X) = -0.001 \mp 0.003,$$

where f_{zz} is the symmetrized g shift introduced in Appendix A.

Using the values of J_{00}, $J_{1-1}\cos_{1-1}$, and J_{11} obtained from measurements of J_{00}', Eq. (22) yields

$$\delta H_1^{(2\mathrm{nd})} = \left(\frac{-|J_{10}|^2}{4g_1\beta h\nu} + \frac{19}{\cos^2\phi_{1-1}} - 1.1 \right) \text{G}, \quad (36)$$

in which the 1.1 G is the contribution from J_{11}. If J_{10} is assigned the dipolar value listed in Table III and ϕ_{1-1} is assumed zero, Eq. (36) yields 15.5 G, a value in excellent agreement with experiment. However, J_{10} could be twice the dipolar value without giving disagreement with experiment. More alarming is the possibility that ϕ_{1-1} is far from zero and J_{10} is large enough to cancel the increased contribution from the J_{1-1} term. This possibility can be limited quite sharply by the centroid shift of the Y-X spectra for which the g value of the observed resonance is the largest of the two. The shift is given by Eq. (23). For an observing frequency of 37 GHz, the result is

$$\delta H_2^{(2\mathrm{nd})} = -\left(\frac{|J_{01}|^2}{4g_2\beta h\nu} + \frac{8.3}{\cos^2\phi_{1-1}} + 0.12 \right) \text{G}. \quad (37)$$

Note that all of the terms are additive. It would be better to use the centroid shifts at both 37 and 16 GHz so as to obtain the g shift and also have the larger 16-GHz second-order effect available for comparison with the calculation. The overlap of the X-Y and Y-X spectra at 16 GHz reduces the accuracy with which the centroid shift can be determined at the lower frequency to such an extent that the high-frequency measurements are far superior. The lack of sensitivity of the value of $g_{11}(Y)$ to diamagnetic constituents suggest that $f_{zz}(Y)$ for the Y-X pairs in LZN is less than 0.001, which would produce a centroid shift of only 0.5 G at 37 GHz. Assuming $f_{zz}(Y)$ to be zero, the dipolar result for J_{01} and $\phi_{1-1}=0$, (37) yeilds −9.0 G. The experimental value is −9±5 G. This result limits J_{01} to within a factor of three of the dipolar value and gives $\phi_{1-1}=0\pm35°$. This analysis demonstrates the lack of sensitivity of the high-field spectra to the antisymmetric part of the interaction. In Sec. IV, it is shown that the antisymmetric terms are expected to be small.

The centroid shifts with the field perpendicular to the symmetry axis are not sensitive to the antisymmetric part of the interaction, but they provide useful checks and interesting information on the changes in the g

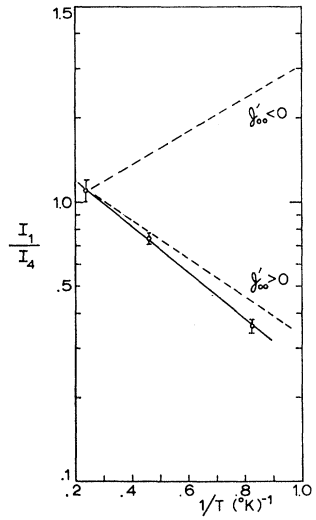

FIG. 9. The temperature dependence of the relative intensity of the high- and low-field components of the X-Y spectrum of LZN at 16 GHz. The two dashed lines have the theoretical values of the slope corresponding to the signs of J_{00} indicated. More dramatic results can be obtained at 37 GHz, as may be surmised by inspection of the relative intensity of high- and low-field components in Figs. 3 and 5, which were taken at 4.2°K.

TABLE IV. Some of the symmetrized changes in the g tensor for the members of Co^{2+} pairs in the double nitrates. Omissions in the table correspond to cases in which the data was not adequate to establish a value, but none of the omitted values were as large as 0.01. The values of f_{zx} and f_{zy} are not tabulated, but they were also established to be less than 0.01 in every case.

	f_{zz}	$\frac{1}{2}(f_{xx}-f_{yy})$	$\frac{1}{2}(f_{xx}+f_{yy})$	f_{xy}
		X Ion of X-Y		
LZN	−0.001 ±0.003	...	...	0.013 ±0.003
LMN	−0.007 ±0.003	...	...	0.03 ±0.02
		Y Ion of X-Y		
LZN	0.000 ±0.005	0.0005 ±0.0005	0.0015 ±0.0010	0.0011 ±0.0005
LMN	0.000 ±0.005	0.0010 ±0.0005	0.004 ±0.001	0.0020 ±0.0005
		X Ion of X-X		
LZN	0.06 ±0.03	...	−0.03 ±0.02	...
LMN	−0.27 ±0.03	...	+0.14 ±0.02	...

tensor. The centroid shifts for the Y-X spectrum obtained from the data in Fig. 6 are plotted in Fig. 10. The solid line represents the theoretical values of the second-order effect. It is apparent that some g-shift effects are present. A change of 0.001 in the effective g value corresponds to a 5 G displacement on this graph. The values obtained for all g shifts are summarized in Table IV. The tensor f_{ij} is defined in Appendix A. The tensor is referred to a set of Cartesian axes for which the z axis is the symmetry axis and the x axis is defined by $\phi=0°$. The element f_{xy} is the one most precisely defined by the experiments since it produces a phase shift in the ϕ dependence of the high-field set relative to that of the low-field set, as was mentioned in the discussion of Fig. 6. The analysis of this data is given in Appendix A. The effect of f_{xz} and f_{yz} are also discussed in the Appendix. For reasons discussed in Appendix A, it was possible to establish only upper limits for f_{xz} and f_{yz}, and these are given in the heading of Table IV. In general, the results for g shifts are not so precise or complete as they might be made. The effort required for further improvement does not seem justified by their minor importance.

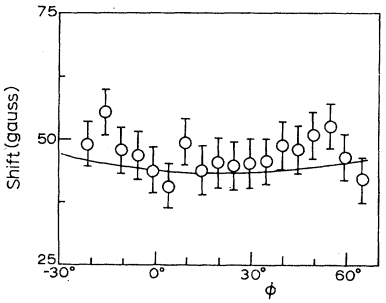

FIG. 10. The centroid of the Y-X pairs relative to the isolated Y ion resonance for directions in the basal plane. The solid line is the calculated shift from the second-order effects of the spin-spin interaction.

C. More Distant Pairs

For the magnetic field along the symmetry axis one additional pair spectrum could be observed for both the X-Y and Y-X. That spectrum near the X spectrum is split ±27 G and is interpreted as the pair with a Y ion which is the fourth nearest neighbor of the X ion. This identification is made on the basis of the dipolar spin-spin interaction that is listed in Table I. The spectrum near that of the Y ion is shifted up and down by approximately 25 G and is interpreted as the closest Y-Y pair on the basis of the dipolar values listed in Table I. Despite the fact that these are similar ions, the hyperfine structure is a simple eight line pattern because the values of all of the spin-spin interaction constants other than J_{00} are very much smaller than A. For the dipolar interaction the ratio of J_{1-1} to A is only 0.017. The effects of all other pairs are too small to observe.

IV. INTERPRETATION IN TERMS OF IONIC PROPERTIES

A. Spin-Spin Interaction

The values of the $J_{mm'}$ produced by a dipolar interaction are

$$J_{00}{}^{(d)}=(\beta^2/r^3)g_{\parallel}(1)g_{\parallel}(2)(1-3\cos^2\Theta), \quad (38a)$$

$$J_{1-1}{}^{(d)}=-(\beta^2/r^3)g_{\perp}(1)g_{\perp}(2)(1-\tfrac{3}{2}\sin^2\Theta), \quad (38b)$$

$$J_{11}{}^{(d)}=-(3\beta^2/2r^3)g_{\perp}(1)g_{\perp}(2)\sin^2\Theta, \quad (38c)$$

$$J_{10}{}^{(d)}=(3\beta^2/\sqrt{2}r^3)g_{\perp}(1)g_{\parallel}(2)\sin\Theta\cos\Theta, \quad (38d)$$

and

$$J_{01}{}^{(d)}=(3\beta^2/\sqrt{2}r^3)g_{\parallel}(1)g_{\perp}(2)\sin\Theta\cos\Theta, \quad (38e)$$

where Θ is the angle between the interionic axis and the symmetry axis and r is the distance between the two ions. If the interionic axis and the trigonal axis define the plane $\phi=0$, then $\phi_{1-1}=\phi_{11}=\phi_{10}=\phi_{01}=0°$. Extensive studies of magnetic interactions in the double nitrate crystals that are completely dipolar have established that the plane which includes the trigonal axis and bisects the side of the hexagonal plate is the plane which contains the interionic axis for the nearest-neighbor X-Y pairs.[10,11] The dipolar values for the X-Y interaction are listed in Table III.

In the last section, it was shown that the experimental data were consistent with all of the antisymmetric interaction being of dipolar origin. If we assume that this is true and assume the most favorable values for ϕ_{11} and $\bar{\phi}$ that is allowed by the ambiguity of multiples of 60°, one obtains the residuals listed in the third

[10] J. W. Culvahouse, W. P. Unruh, and R. C. Sapp, Phys. Rev. 121, 1370 (1961).

[11] F. W. Addis, Ph.D. thesis, University of Kansas, 1968 (unpublished).

column of Table III. The residual interaction is described quite accurately by a nondioplar interaction

$$\mathcal{H}_{12}^{(nd)}=K_{11}S_1^zS_2^z+K_\perp(S_1^xS_2^x+S_1^yS_2^y), \quad (39)$$

where $K_{11}=J_{00}^{(nd)}$ and $K_\perp=-J_{1-1}^{(nd)}$. For LZN,

$$K_{11}=0.1899\pm0.002 \text{ cm}^{-1}$$

and

$$K_\perp=0.0774\pm0.002 \text{ cm}^{-1}.$$

The corresponding values for LMN are 0.1794 and 0.0738 cm^{-1} with comparable errors. The only significant disagreement with the experimental data is the residual for J_{1-1}, which is 0.003 cm^{-1}, about twice the experimental error. A part of this can be explained by the effect of g shifts and is considered again in the discussion of those effects below.

B. Projection of Exchange between Ionic Spins

The form of the nondipolar interaction (39) and the ratio of $(K_{11}/K_\perp)$ for the X-Y interaction can be reproduced with considerable precision by assuming that there is an isotropic exchange between the ionic spins $\mathfrak{S}$,

$$\mathcal{H}_i^{(ex)}(1,2)=K_i\mathfrak{S}(1)\cdot\mathfrak{S}(2), \quad (40)$$

which is projected onto the eigenstates of the effective spin. This assumption has been applied to the cobalt Tutton salt, $Co(NH_4)(SO_4)_2\cdot6H_2O$, by Uryû[12,13] to explain the bulk-magnetic and thermal properties of this material. The concept has not been tested with the precision provided by the pair data of Table III.

The evaluation of the matrix elements of (40) in a product representation of the eigenstates of S_1^z and S_2^z yields

$$K_{11}=\tfrac{1}{4}g_{s11}(X)g_{s11}(Y)K_i \quad (41a)$$

and

$$K_\perp=\tfrac{1}{4}g_{s\perp}(X)g_{s\perp}(Y)K_i, \quad (41b)$$

in which g_s is the part of the g tensor in the spin Hamiltonian which arises from the ionic spin. If $|\pm\rangle$ designate the eigenstates of S^z, one has the definitions

$$\tfrac{1}{2}g_{s11}=\langle+|2\mathfrak{S}_z|+\rangle \quad (42a)$$

and

$$\tfrac{1}{2}g_{s\perp}=\langle+|\mathfrak{S}_+|-\rangle. \quad (42b)$$

The values of g_{s11} and $g_{s\perp}$ are tabulated in Table II. The values for LZN were obtained from the wave functions given by Olsen and Culvahouse,[4] and the other values were derived from those by using perturbation theory to calculate the effect of a small additional trigonal perturbation.

The values deduced for K_i are given in Table V. Besides the results for LMN and LZN, there is an entry for LZN in which most of the water of hydration (80%) was replaced by heavy water. The incomplete replacement of the light water resulted in strains which broadened the lines and reduced the accuracy of the measurements. J_{00} could be determined with useful precision; from that, a value of K_i was deduced. The K_i values for LMN and LZN agree very well, but it appears that deuteration may have reduced K_i by 5%.

TABLE V. The measured anisotropy of the nondipolar part of the X-Y interactions in LZN and LMN and the values for this ratio obtained by projection of an isotropic exchange between ionic spins. The value of K_i for the ionic exchange required to fit the data is given in the last column.

	$\frac{K_{11}}{K_\perp}$	$\frac{g_{s11}(X)g_{s11}(Y)}{g_{s\perp}(X)g_{s\perp}(Y)}$	$\frac{g_{11}(X)g_{11}(Y)}{g_\perp(X)g_\perp(Y)}$	K_i (cm^{-1})
LZN	2.45 ±0.08	2.62	3.19	0.0438 ±0.0010
LMN	2.46 ±0.08	2.43	2.87	0.0437 ±0.0010
LZN(D_2O)	...	...	...	0.0417 ±0.0010

In the second and third columns of Table V, the experimental and theoretical values of the ratio $(K_{11}/K_\perp)$ are compared. The agreement is excellent for LMN and only 2% outside the probable error in the experimental value for LZN. The values g_s for the wave functions need to be changed only 0.5% to produce a change in the theoretical ratio which would lead to agreement within the experimental error for both cases. The conclusion must be that the projection of ionic exchange yields excellent agreement with experiment. In the fourth column, we tabulate the ratio $(K_{11}/K_\perp)$ that would be obtained if the total g tensor were used in Eqs. (41) instead of g_s.

This anslysis is now extended to the X-X interaction which was reported in Ref. 5. The nondipolar part of the interaction in LMN can be described by (39) with $K_{11}=0.064\pm0.003$ cm^{-1} and $K_\perp=0.040\pm0.003$ cm^{-1}. The g factors were found to be isotropic within 0.5% and it follows that the ratio of g_{s11} to $g_{s\perp}$ is unity within 1%. The projection of isotropic exchange between ionic spins gives $K_{11}/K_\perp=1.00\pm0.02$, but the experimental value is 1.60 ± 0.14. This result constitutes a clear refutation of the method of projecting isotropic exchange between ionic spins as a general method for Co^{2+}.

C. Projection of Orbital Exchange

There are now a number of calculations which show explicitly that the projection of an isotropic exchange between ionic spins onto the effective spin states is a realistic procedure only in very restricted situations.[14–17] The only case in which the ionic properties alone justify the method is that of an orbital singlet state separated

[12] N. Uryû, J. Phys. Soc. Japan **11**, 770 (1956).
[13] N. Uryû, J. Phys. Soc. Japan **16**, 2139 (1961).
[14] J. H. Van Vleck, Rev. Mat. Fis. Teórica (Tucumán, Argentina), **14**, 189 (1962).
[15] Peter M. Levy, Phys. Rev. **135**, A155 (1964).
[16] R. J. Elliott and M. R. Thorpe, J. Appl. Phys. **39**, 802 (1968).
[17] Peter M. Levy, Phys. Rev. **177**, 509 (1969).

from other orbital states by an energy large in comparison with the exchange interaction and the spin-orbit interaction. In this case the effective spin and the ionic spin are identical and the effects of the spin-orbit interaction can be formulated in a perturbative treatment which leads to the well-known pseudodipole and pseudoquadrupole effects (the latter only if the spin is greater than one-half).[18] These anisotropic effects arise from the same matrix elements as do the small deviations of the g factors from the free-electron value. Clearly the situation for Co^{2+} does not satisfy these criteria at all, and the success of the projection of isotropic exchange between ionic spins for the X-Y interaction is perhaps more surprising than the failure for the X-X.

The situation for Co^{2+} is somewhat similar to that for rare-earth ions. The octahedral crystal field leaves a triply degenerate $^4T_1$ state lowest; and the effects of the trigonal crystal field and the spin-orbit interactions are comparable.[19] The simplifying features of the X-Y interaction appear to emerge quite naturally from the form of the Co^{2+} wave functions and the character of the hydrogen bonding between the X and Y complexes. To show this, it is necessary to begin with the more fundamental concept of an exchange potential between individual electrons, the spin-dependent part of which is

$$\mathcal{H}_{ex}=\sum_{i,j} J_{ij}\mathbf{s}_i\cdot\mathbf{s}_j, \tag{43}$$

where i and j run over the electrons in ions 1 and 2. This is only an effective Hamiltonian designed to reproduce the effect of the nonlocalizability of the electrons within a manifold of states with a one-to-one correspondence to the true eigenstates, but for which electrons are on specified atoms, their "home-bases." Herring[20] has shown how this approach can be given a much more general basis than that provided by the Heitler-London theory. He has not given so much attention to the case in which there is orbital degeneracy, with the result that spin-orbit interactions are important; but it appears that the same concepts can be applied and this has been assumed in even the most sophisticated calculations.

Van Vleck[14] pointed out that J_{ij} in (43) must depend on the orientation of the orbitals occupied by electrons i and j. Levy[17] has recently shown how explicit evaluation leads to such dependencies. Other authors[16] have assumed (presumably on the basis of general symmetry arguments) that if the integration over the angular coordinates of electrons i and j is left undone, the angular dependence will be in the form of a bilinear product of spherical harmonics in the polar angles of the two electrons. Such a series can be replaced with an equivalent one involving the irreducible tensor operators formed from l_i and l_j:

$$\mathcal{H}_{ex}=\sum_{kk'}\sum_{qq'}\sum_{ij} J_{kk'}{}^{qq'}T_{kq}(l_i)T_{k'q'}(l_j)\mathbf{s}_i\cdot\mathbf{s}_j. \tag{44}$$

The calculation by Levy[15] gives this result, but is more explicit and exhibits relations among the $J_{kk'}{}^{qq'}$. The fact that k and k' must be even and less than $2l+1$ (if l is the orbital angular momentum of the electrons) follows from very general considerations. Elliott and Thorp[16] outline the procedure by which suitable recouplings of angular momenta may be used to obtain operator forms suitable for L-S manifolds, J manifolds, or $\mathfrak{L}$-S manifolds in the cases for which crystal field interactions give rise to effective orbital angular momentum operators $\mathfrak{L}$.

For our purposes, it is more direct to write the exchange Hamiltonian in another form that is equivalent to (44):

$$\mathcal{H}_{ex}=\sum_{\alpha\beta\gamma\delta}\sum_{ij} k_{\alpha\beta\gamma\delta}G(\eta_i,\alpha,\beta)G(\eta_j,\gamma,\delta)\mathbf{s}_i\cdot\mathbf{s}_j, \tag{45}$$

where α, β, γ, and δ run over all of the orbital states, and the orbital operator $G(\eta_i,\alpha,\beta)$ is defined by the matrix elements between one electron orbitals. For electron i

$$\langle\alpha'|G(\eta_i,\alpha,\beta)|\beta'\rangle=\delta_{\alpha\alpha'}\delta_{\beta\beta'}; \tag{46}$$

e.g., it is zero except for electron i in the orbital α in the bra and β in the ket. It is easy to show from the orthogonality relation for the vector coupling coefficients[21] that, for a complete set of orbitals of angular momentum l,

$$G(l_i,m,m')=\sum_{k,q}(2k+1)\frac{\langle lm|T_{kq}|lm'\rangle T_{kq}(l_i)}{|\langle l\|T_{kq}\|l\rangle|^2}, \tag{47}$$

which demonstrates the equivalence of (44) and (45). The parameters $k_{\alpha\beta\gamma\delta}$ arise in the evaluation of exchange and transfer integrals. For potential exchange[22]

$$k_{\alpha\beta\gamma\delta}=\int\int u_\alpha^*(\mathbf{r}_1)u_\delta(\mathbf{r}_1-\boldsymbol{\tau})\frac{e^2}{|\mathbf{r}_1-\mathbf{r}_2|}\times u_\gamma^*(\mathbf{r}_2-\boldsymbol{\tau})u_\beta(\mathbf{r}_2)dV_1dV_2, \tag{48}$$

which are terms that arise from considering electron interchanges between orbital states which involve a mixture of the basis orbitals. For kinetic exchange

$$k_{\alpha\beta\gamma\delta}=2b_{\alpha\delta}b_{\gamma\beta}/U, \tag{49}$$

where $b_{\alpha\beta}$ is the electron transfer integral from orbital α on ion 1 to orbital β on ion 2, and U is the promotion energy involved in the transfer. From (48) and (49), it is clear that

$$k_{\alpha\beta\delta\gamma}=k_{\beta\alpha\delta\gamma}^* \tag{50}$$

[18] J. H. Van Vleck, Phys. Rev. **52**, 1178 (1937).
[19] A. Abragam and M. H. L. Pryce, Proc. Roy. Soc. (London) **A206**, 173 (1951).
[20] C. Herring, in *Magnetism*, edited by G. T. Rado and H. Suhl (Academic Press Inc., New York, 1966), Vol. II B.
[21] Reference 6, pp. 47 and 75.
[22] P. W. Anderson, in *Magnetism*, edited by G. T. Rado and H. Suhl (Academic Press Inc., New York, 1963), Vol. I.

and further relations may be derived from the considerations of time inversion symmetry. If the orbitals on the two ions are related by an inversion center, one would also have

$$k_{\alpha\beta\gamma\delta}=k_{\gamma\delta\alpha\beta}. \tag{51}$$

The explicit calculations of Levy show that the number of independent constants required to describe the exchange may be less than the number of independent $k_{\alpha\beta\gamma\delta}$. The only chance of a really simple description of exchange between orbitally degenerate states arises when only a few of the $k_{\alpha\beta\gamma\delta}$ are important.

For ions of the first transition group in a strong cubic crystal field, the most natural set of orbitals are the e_g and t_{2g} representations of the cubic group formed by the d orbitals. We follow Griffith[23] in the notation for the representations of the cubic group and in using lower case for orbitals, upper case for ionic terms. For Co^{2+} in an octahedral crystal field, the orbital triplet T_1 is lowest and the ionic spin is $\frac{3}{2}$. The states are designated $^4T_1(m)$ where $m=\pm1,0$ represents the eigenvalue of the effective angular momentum operator $\mathfrak{L}_z$, introduced by Abragam and Pryce.[24] We use z' to designate one of the fourfold axes of the octahedron. Both of the three-dimensional representations T_1 and T_2 are isomorphic with a set of p orbitals, and the matrix elements of $\mathbf{L}$ within the triplets are proportional to those of $\mathfrak{L}$; thus the components of both T_1 and t_{2g} are identified by the effective quantum number m.

If the octahedral field is very strong, the ground state of Co^{2+} corresponds to the three holes in the configuration $e_g^2t_{2g}$. In weaker fields there is some $e_gt_{2g}^2$ configuration admixed into the ground states

$$|{}^4T_1,m,\mathfrak{S},\mathfrak{S}_z\rangle=\cos\chi|e_g^2t_{2g},{}^4T_1,m,\mathfrak{S},\mathfrak{S}_z\rangle +\sin\chi|e_gt_{2g}^2,{}^4T_1,m,\mathfrak{S},\mathfrak{S}_z\rangle. \tag{52}$$

If the crystal field completely dominates the coulomb interactions between the electrons on the ion, $\sin\chi=0$; and in the limit of a very weak crystal field, $\sin\chi=-1/\sqrt{5}$. The appropriate value of $\sin\chi$ for $(Co\cdot6H_2O)^{2+}$ can be found from the coulomb integrals and crystal field splittings given by Griffiths.[23] Values more directly related to experimental results can be found from the fitting of the g values for the ground doublet. This fitting implies a value for α in the relation $L_z=\alpha\mathfrak{L}_z$. An expression for α in terms of χ can be found from the determinantal forms of the states in (52):

$$|e_g^2t_{2g},{}^4T_1,m,\tfrac{3}{2},\tfrac{3}{2}\rangle=\{\theta^+\epsilon^+t_{2g}(m)^+\}_{\rm det}, \tag{53a}$$

$$|e_g^2t_{2g},{}^4T_1,\pm1,\tfrac{3}{2},\tfrac{3}{2}\rangle=-\tfrac{1}{2}\{\theta^+t_{2g}(\pm1)^+t_{2g}(0)^+\}_{\rm det} -\tfrac{1}{2}\sqrt{3}\{\epsilon^+t_{2g}(0)^+t_{2g}(\mp1)^+\}_{\rm det}, \tag{53b}$$

and

$$|e_gt_{2g}^2,{}^4T_1,0,\tfrac{3}{2},\tfrac{3}{2}\rangle=\{t_{2g}(1)^+t_{2g}(-1)\theta^+\}_{\rm det}, \tag{53c}$$

[23] J. S. Griffith, *The Theory of Transition-Metal Ions* (Cambridge University Press, London, 1961).

[24] A. G. Taylor, L. C. Olsen, D. K. Brice, and J. W. Culvahouse, Phys. Rev. **152**, 403 (1966).

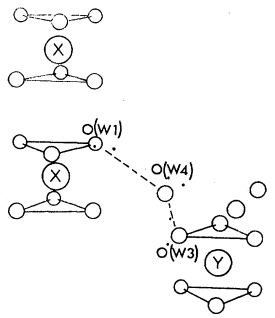

FIG. 11. The water octahedra about the X and Y ions and the hydrogen bonds which bond the oxygen of the X complex and of the Y complex to the oxygen of a noncoordinated water molecule. The oxygen ions are labeled with the notation of Ref. 1.

where the + superscripts imply that the orbital spin is up, and we have used the coupling tables given by Griffith. From these functions we find

$$\alpha=-\cos^2\chi+\tfrac{1}{2}\sin^2\chi+2\sin\chi\cos\chi. \tag{54}$$

Olsen[4] found $\alpha=-1.374$ for the X ion in LZN which corresponds to $\sin\chi\approx\frac{1}{4}$. The value of α is not the same for all components of $^4T_1$ when the trigonal field of the Y ion is taken into account, but the average value is essentially the same and the variation from $^4T_1(\pm1)$ to $^4T_1(0)$ is not large. We shall not concern ourselves with these small effects as we shall show that the admixture of the $e_gt_{2g}^2$ configuration is of minor importance in the model which we adopt. We therefore discuss a pure $e_g^2t_{2g}$ configuration first and turn to the complications of the admixture later.

The important property of the $e_g^2t_{2g}$ configuration is that it contains a half-filled e_g shell. The consequence of this is reflected in the determinantal form (53a), from which it is apparent that the parent of the $^4T_1$ state is the singlet A_2 formed from the e_g states. It is therefore obvious that if only the e_g orbitals were involved in exchange, the exchange problem would be equivalent to that for an orbital singlet. More formally, this result follows from a demonstration that the matrix elements of

$$\sum_i G(\eta_i,\alpha,\beta)\mathbf{s}_i$$

are just those of $\mathfrak{S}/3$ within the $e_g^2t_{2g}$ configuration for α and β equal to θ or ϵ.

Ignoring the complications of configuration admixture, the simple hypothesis of e_g exchange only explains the nature of the X-Y interaction. The validity of this hypothesis is suggested by the nature of the hydrogen bonding between the X and Y orbitals. These bonds terminate on the oxygen ions of the complexes, and the e_g orbitals are most effective in forming σ bonds with the oxygen ions. The hydrogen bonds that are most likely to be involved in the X-Y interaction are those which bond oxygen ions of the X and Y complexes to the oxygen of a noncoordinated water molecule. These are the bonds O($W1$)—H($1W1$)—O($W4$) and

O($W3$)—H($2W2$)—O($W4$) listed in Table IX of Ref. 1 and illustrated in Fig. 1 of that paper. A schematic picture of these bonds is given in our Fig. 11. There is another set of bonds which bind oxygens of the X and Y complexes to a common nitrate ion, but the exchange path appears more tenuous than the one depicted in Fig. 11. Both exchange paths should involve e_g orbitals more than t_{2g} orbitals and lead to the observed results.

If the z' axis for the X ion is taken as that fourfold axis in the direction of O($W1$) and that on the Y ion is taken as the fourfold axis in the direction of O($W3$), then $\theta\sim(3z'^2-r^2)$ is the only orbital involved in σ bonding to the oxygens in the primary exchange path. For this choice of representations the exchange between ionic spins is given by (40) with

$$K_i=\tfrac{1}{9}k_{\theta\theta\theta\theta}. \tag{55}$$

For other choices of axes, the θ and ϵ orbitals are mixed; and if the second exchange path is considered, both θ and ϵ orbitals must contribute for any choice of axes.

If it is assumed that exchange between e_g and t_{2g} orbitals is insignificant, the effect of the $e_g t_{2g}^2$ configuration admixture is very slight because all of the corrections are of the order of $\sin^2\chi\approx 0.06$. We illustrate this effect by working out the exchange for a model in which only the θ orbital is involved as suggested by the arguments in the preceding paragraph, but assuming an arbitrary value for χ. Using (52) and (53), one finds

$$\langle {}^4T_1,\pm1,\tfrac{3}{2},\tfrac{3}{2}|\sum_i G(\eta_i,\theta,\theta)|{}^4T_1,\pm1,\tfrac{3}{2},\tfrac{3}{2}\rangle =\tfrac{1}{3}-\tfrac{1}{4}\sin^2\chi, \tag{56a}$$

$$\langle {}^4T_1,0,\tfrac{3}{2},\tfrac{3}{2}|\sum_i G(\eta_i,\theta,\theta)|{}^4T_1,0,\tfrac{3}{2},\tfrac{3}{2}\rangle=\tfrac{1}{3}, \tag{56b}$$

and there are no off-diagonal elements. From the Wigner-Eckart theorem, the operator identity

$$\sum_i G(\eta_i,\theta,\theta)\equiv\tfrac{1}{3}(1-\tfrac{3}{4}\sin^2\chi\mathfrak{L}_{z'}^2) \tag{57}$$

is valid for the configuration and the restricted set of states. That only $\mathfrak{L}_{z'}$ is involved in (57) corresponds to the fact that the exchange interaction between ionic spins would still have axial symmetry if the complexes had cubic symmetry. It is essential that the effect of the trigonal splitting as well as the spin-orbit interaction be included in the ground states for which the exchange is calculated. This is easily done with $\mathfrak{L}$ referred to the trigonal axis.[19,23] It is most convenient to transform (57) to this axis by the relation

$$\mathfrak{L}_{z'}=(\mathfrak{L}_x+\mathfrak{L}_y+\mathfrak{L}_z)/\sqrt{3}, \tag{58a}$$

which yields

$$\sum_i G(\eta_i,\theta,\theta)\equiv(1-\tfrac{1}{2}\sin^2\chi) -[(1-i)/24](\sin^2\chi)(\mathfrak{L}_z\mathfrak{L}_+ +\mathfrak{L}_+\mathfrak{L}_z) -(i/24)(\sin^2\chi)\mathfrak{L}_+\mathfrak{L}_+ +(\text{adjoint terms}). \tag{58b}$$

The lowest-lying pair of eigenstates of the combined trigonal field and spin-orbit interaction are

$$|\pm,X\rangle=a_x|{}^4T_1,\ -1,\tfrac{3}{2},\tfrac{3}{2}\rangle+b_x|{}^4T_1,0,\tfrac{3}{2},\tfrac{1}{2}\rangle +c_x|{}^4T_1,1,\tfrac{3}{2},-\tfrac{1}{2}\rangle \tag{59}$$

and a similar function for the Y ion. The values of a, b, and c for both ions are given by Olsen.[4] Using (45), (58b), and (59), the spin-spin interaction parameters due to exchange are given by

$$\tfrac{1}{4}J_{00}=|\langle+,X|\langle+,Y|\mathfrak{IC}_{ex}|+,X\rangle|+,Y\rangle|, \tag{60a}$$

$$-\tfrac{1}{2}J_{1-1}=|\langle+,X|\langle-,Y|\mathfrak{IC}_{ex}|-,X\rangle|+,Y\rangle|, \tag{60b}$$

$$\tfrac{1}{2}J_{11}=|\langle+,X|\langle+,Y|\mathfrak{IC}_{ex}|-,X\rangle|-,Y\rangle|, \tag{60c}$$

$$-J_{10}/2\sqrt{2}=|\langle+,X|\langle+,Y|\mathfrak{IC}_{ex}|-,X\rangle|+,Y\rangle|. \tag{60d}$$

Finite values are obtained for J_{11} and J_{10}; but for $\sin\chi=\frac{1}{4}$ the values are all less than 1% of J_{00} and hence less than 0.002 cm^{-1}. The largest effect is the reduction of the value of J_{00} and J_{1-1} by a factor of 0.94. An accuracy of 1% is retained for the θ-only model by assuming isotropic exchange between ionic spins with

$$K_i=(0.94/9)k_{\theta\theta\theta\theta}. \tag{61}$$

The dependence of the projection operators on $\mathfrak{L}$ introduces anisotropy beyond that related to g_s and their presence also leads to antisymmetry in the exchange (e.g., $J_{10}\neq J_{01}$) if the wave functions (59) are different for the two ions. The degree of asymmetry will be quite unrelated to that in the dipole-dipole interaction. There are other small corrections from the spin-orbit coupling to orbital states outside the triplet, and these are nonsymmetric as well as anisotropic. There is a more subtle source of antisymmetric interactions which could exist even when the complexes are identical. Unless there is an inversion center between the two ions, the transfer integrals could still be antisymmetric for interchange of ionic indices because of effects in the region between the complexes This question does not arise for the model which can be reduced to exchange between the θ orbitals alone. It is apparent that sizes of the antisymmetric effects expected for our model are well below those that could have been detected in the experiments.

There is another minor effect which has been thus far ignored. The strain induced changes in the g tensors for an isolated pair reflect changes in the ionic wave functions. The effects on the measured interaction are easily calculated for the projection of (40) onto the effective spin states. The result can be stated in terms of the changes in the tensor g_s. One finds that there is a small J_{11} and ϕ_{1-1} is different from zero (antisymmetry). The effects are all less than 1%. There is a similar, but purely experimental effect which arises from our assumption that the quantization axis was given by the g tensor of the isolated ion. Spurious terms are thereby introduced which are of the same order of magnitude

as the real changes in the spin-spin interaction produced by the changes in the wave functions. All of these effects are of the same order as some of the higher-order perturbation effects which were ignored in the treatment of the phenomenological Hamiltonian (2). Finally, we note that the strain might have some effect on the transfer integrals. The similarity of the value of K_i for pairs in LZN and LMN suggest that this effect is very slight. The different K_i for the deuterated material may reflect just such an effect.

For the X-X interaction the bonding situation is in sharp contrast to that for the X-Y pairs. There are no apparent linkages between the oxygen ions nor any which join them to a common ion. In a general way, this probably accounts for the fact that the nondipolar part of the X-X interaction is less than that for the X-Y interaction despite the interionic separations of 4.99 and 7.14 A, respectively. If only e_g exchange were involved in the X-X interaction, the projection of isotropic exchange between ionic spins would be accurate to a few percent. As noted in the preceding subsection, the projection of (40) gives an isotropic interaction in the effective spin whereas the experiment requires $K_{\parallel}/K_{\perp}=1.60$. This implies that the t_{2g} orbitals must be significantly involved.

The trigonal symmetry retained by the pair allows one to use symmetry to reduce the number of independent transfer integrals to four. Still the data for Co^{2+} is not sufficient to narrow the spectrum of possibilities appreciably further except for the elimination of a pure e_g model as noted in the last paragraph. Of the four independent integrals permitted by trigonal symmetry, one of them is between e_g and t_{2g} orbitals. This means that cross terms between the $e_g^2t_{2g}$ and $e_gt_{2g}^2$ configurations are possible on the basis of gross symmetry arguments.

The amount of anisotropy in the X-X interaction can be explained within the general context of the model. This is demonstrated by a calculation which assumes transfer between the states $t_{2g}(\pm 1)$, where ± 1 is now the eigenvalue of $\mathfrak{L}_z$ rather than $\mathfrak{L}_{z'}$ as in earlier paragraphs. The calculation yields $K_{\parallel}/K_{\perp}=82/11$. A more complete analysis may be justified when there is data for ions with different configurations.

D. Interpretation of the G Shifts

For the X-X pairs the symmetry is still trigonal and the g shifts are described by $f_{\parallel}$ and $f_{\perp}$ which are themselves related by the constraint[3]

$$g_{\parallel}+2g_{\perp}=12.97\pm 0.03.$$

It has been found that the value of $g_{\parallel}$ (and therefore $g_{\perp}$) for Co^{2+} in an X site is determined by the diamagnetic ion in the nearest-neighbor site. This has been established by measurements made on the EPR spectra of double nitrate crystals containing 0.05% Co^{2+} and Mg^{2+} mixed with Zn^{2+} in the ratios 1:7 in one case and 7:1 in another. In both cases, two X-ion spectra were observed. The corresponding spin-Hamiltonian parameters were identical to those for LZN and LMN within experimental errors of 0.5%. The relative intensities of the two spectra were very close to 7:1 and the weaker spectrum corresponded to that of the minority ion. It is concluded from this that the spin-Hamiltonian parameters of an ion in the X site are determined by the occupant of the nearest-neighbor X site, and that the g value for an isolated X-X pair of Co^{2+} ions is virtually identical to that of Co^{2+} ions in LCN.

With the magnetic field along the symmetry axis, the only discernable strain effect in the mixed crystals was the extra X ion spectra. This is in agreement with the results on the g shifts of X-Y pairs which showed that $g_{\parallel}$ for the members of an X-Y pair is essentially the same as for isolated ions. With the magnetic field perpendicular to the symmetry axis the X-ion spectrum of the mixed crystals was considerably broader than that in pure crystals, and the amount of broadening increased from the high- to low-field hyperfine components. This sort of variation is the signature of strain effects because of concomitant changes in the g and A tensors which tend to produce cancelling shifts on the high-field side and additive shifts on the low-field side, an effect directly analogous to the variation of the relaxation time from the low- to high-field components.[3] The noticeable broadening for this field direction is in accord with the rather large value of f_{xy} observed for the X ion of an X-Y pairs. Verification of similar effects on the Y-ion spectrum with the field perpendicular to the symmetry axis are more difficult. The spectrum is highly sensitive to the field direction, and even good quality pure crystals show effects which appear to be due to a mosaic structure.

The g values for X ions in LMN, LCN, and LZN appear to be well correlated with the ionic radii of the neighboring cation, and it is reasoanble to assume that the changes in the g factor arise solely from changes in the ligand field induced by the accommodation of the ions. There is no evidence of a multipole interaction between the paramagnetic ions. It is a bit more difficult to establish the corresponding result for the X-Y pairs. One surprising feature in that case is the similarity of f_{xy} for LZN and LMN. One would anticipate that the Co ion produces much more strain in the LMN lattice than in the LZN lattice, and this is apparently true for the X-X pairs where the shift produced by substituting Co for Mg is from 5 to 15 times larger than that produced by the substitution of Co for Zn. This contrast tends to suggest that a part of the shift for X-Y pairs might be due to electric multipole interactions between cobalt ions; but comparison of the relative size of f_{xy} for the X and Y members of a pair leads to an argument against the electric multiple interaction. This argument is based on the fact that the changes in the g tensor arising either from strain or an electric multipole inter-

action with a paramagnetic neighbor can be represented as the result of a change V' in the crystal field. Taylor *et al.*[24] have given expressions for the change in the g tensors, and from those results one finds

$$\frac{[f_{xy}]_X}{[f_{xy}]_Y}=\frac{[\beta_{xx}'\,\mathrm{Im}(M_3)]_X}{[\beta_{xx}'\,\mathrm{Im}(M_3)]_Y}\cong 2.5\frac{[\mathrm{Im}(M_3)]_X}{[\mathrm{Im}(M_3)]_Y}, \quad (62)$$

where M_3 is the matrix element of V' between the states $T_1(\pm 1)$, where the quantum numbers in the parentheses are those of $\mathfrak{L}_z$. The experimental value of the ratio on the left-hand side of (62) is approximately 10. Since the wave functions $T_1(m)$ are not significantly different for the X and Y ions, one is forced to conclude that the strain induced potential at the X site is about 4 times greater than at the Y site. A multipole-multipole interaction between the two ions would produce the same effective potential V' at the two sites. On the other hand, strain effects might well be much larger at the X site than at the Y site. The environment of the Y ion is much more firmly held to the rest of the lattice than is that of X ion. Three of the six water molecules in the X complex do not participate in any of the hydrogen bonding which ties the whole structure together. We conclude that a significant multipole-multipole interaction between the X and Y ions is unlikely, but that our understanding to the g shifts is not complete.

V. PROPERTIES OF LCN

In this section, the experimental spin-spin interaction parameters are used to calculate the magnetic and magnetothermal properties of LCN. This exercise provides a valuable check for possible concentration and field dependent interactions, and leads us to a probable structure for the ordered state.

A. Magnetic Susceptibility

The principal values of the susceptibility tensors at temperatures well above the critical point can be written[25]

$$\chi_{\alpha\alpha}=\gamma_{\alpha\alpha}+(C_{\alpha\alpha}/T)[1+(\theta_1)_{\alpha\alpha}/T+(\theta_2)_{\alpha\alpha}/T^2+\cdots], \quad (63)$$

in which $\gamma_{\alpha\alpha}$ is the temperature-independent susceptibility tensor. The Curie constants are given by

$$C_{\alpha\alpha}=\frac{1}{k}\sum_i (R_{i\alpha})^2, \quad (64)$$

where

$$R_{i\alpha}=\tfrac{1}{2}g_{\alpha\alpha}(i) \quad (65)$$

and Greek subscripts are used for Cartesian components referred to the principal axes; i, j, and l are used here and later to designate ions. The other parameters may be calculated from the spin-spin interaction coefficients using formulas given by Daniels[26]:

$$(\theta_1)_{\alpha\alpha}=(-2/C_{\alpha\alpha}k^2)\sum_{(ij)} P_{ij\alpha\alpha}R_{i\alpha}R_{j\alpha} \quad (66)$$

and

$$(\theta_2)_{\alpha\alpha}=(1/12C_{\alpha\alpha}k^2)\{24\sum_{(ij)(jl)\,i\neq l} P_{ij\alpha\beta}P_{jl\beta\alpha}R_{i\alpha}R_{l\alpha}+4\sum_{(ij)}[(P_{ij\alpha\beta})^2(R_{i\alpha})^2+(P_{ij\beta\alpha})^2(R_{j\alpha})^2]-4\sum_{(ij)}(P_{ij\beta\gamma})^2[(R_{i\alpha})^2+(R_{j\alpha})^2]\}, \quad (67)$$

where a summation over bracketed indices means a sum over pairs, the summation convention applies to the Greek subscripts, and

$$P_{ij\alpha\beta}=\tfrac{1}{4}J_{\alpha\beta}(i,j), \quad (68)$$

in which $J_{\alpha\beta}(i,j)$ are the spin-spin interaction constants in Cartesian form.

Eqs. (66) and (67) were evaluated using only the spin-spin interaction between the nearest-neighbor X-X and X-Y pairs. The other interactions contribute an amount that is much less than the experimental uncertainty in the large interactions which lead to a 3% uncertainty in θ_1 and a 6% uncertainty in θ_2. The results are tabulated in Table VI under the heading of calculated values. The values for $C_{\parallel}$ and $C_{\perp}$ listed in that column were calculated using the g values for the X ion listed in Table II for X-X pairs. The results of the mixed crystal experiments described in the last section imply that these are the correct values for the X ion in LCN with an uncertainty of the order of 0.5%. The g values for the Y ion were taken as those tabulated for LZN.

The values obtained by Leask and Wolf[25] from fitting (63) to the measured susceptibility are listed in the third column of Table VI. The agreement appears to be quite poor, but the difficulty is only the one of finding a unique fit to the experimental data. We find that the values of $\chi_{\parallel}$ and $\chi_{\perp}$ calculated from (63) with the constants of Leask and Wolf and our theoretical constants agree within 0.5% over the entire temperature range from 1.1 to 20.4°K if $\gamma_{\parallel}$ and $\gamma_{\perp}$ are assigned the slightly different values listed in column two of Table VI. This is believed to constitute an excellent agreement between the measured susceptibility and that calculated from single-ion and ion-pair data.

B. Magnetic Specific-Heat Tail

Well above the critical point, the magnetic specific heat is described by

$$C_M=(b_M+b_{\mathrm{hyf}})/T^2, \quad (69)$$

in which

$$b_{\mathrm{hyf}}=(k/12)I(I+1)\sum_i (A_i^2+2B_i^2) \quad (70)$$

[25] M. J. M. Leask and W. P. Wolf, Proc. Phys. Soc. (London) **A81**, 252 (1963).

[26] J. M. Daniels, Proc. Phys. Soc. (London) **A66**, 673 (1953).

is the contribution of the hyperfine splitting, and

$$b_M=(1/k)\sum_{(i,j)}\sum_{\alpha\beta}(P_{ij\alpha\beta})^2 \tag{71}$$

is the spin-spin contribution. Reference to Table VI shows that the calculated value is in satisfactory agreement with the calorimetric measurement of Mess *et al.*[27] and the adiabatic susceptibility measurement of Sapp.[28]

C. Transition Temperature and Ordered State

Mess *et al.*[27] have found that the specific heat of LCN is characteristic of a magnetic phase transition at 0.181°K. The temperature dependence of the susceptibility suggest an antiferromagnetic transition. These authors have also reported a total ordering energy of 0.157R cal/g-ion. We show here that these experimental values for the bulk properties are in accord with the measured spin-spin interactions of the pairs.

The Y ions of the double nitrate lattice lie in layers $Y(i)$ perpendicular to the trigonal axis and separated by 11.4 A. These layers are sandwiched between two layers of X ions which are 3.27 A above and below the Y-ion layer. We designate these layers by $X_{\pm}(i)$. The strong and highly anisotropic X-Y interactions are between the ions in $Y(i)$ and $X_{\pm}(i)$. Each Y ion interacts with three X ions in the layer above and with three others in the layer below. This sandwich, X-Y-X, would clearly tend to order with the spins of the X and Y ions antiparallel. Aside from dipolar effects, which we show are not completely negligible, the other major interaction is between the X ions of adjacent sandwiches. Each X ion in the layer $X_+(i)$ interacts rather strongly with the X ion directly along the trigonal axis and lying in the layer $X_-(i+1)$. The total X-X interaction, including the dipolar part, is given by

$$\mathcal{H}(X,X)=J_{00}S_1^zS_2^z-\tfrac{1}{2}J_{1-1}(S_1^+S_2^-+S_1^-S_2^+) \tag{72}$$

with $J_{00}=-0.065$ cm^{-1} (ferromagnetic) and $J_{1-1}=-0.105$ cm^{-1} (antiferromagnetic).

A purely classical calculation in which only the z-z components of the X-Y and X-X interaction are considered would give the energetically favored structure as one with all Y layers ordered with their spins along the z axis in one sense, and the X layers with their spins ordered in the opposite sense. This calculation is unrealistic for two reasons. Firstly, the transverse components of the spin-spin interaction are important; and secondly, the dipolar fields produced by more distant neighbors play an important role. We show presently that second factor is decisive in deciding between the ferrimagnetic structure just proposed and an antiferromagnetic structure. The first factor has a significant effect on the magnitude of the ordering energy.

[27] K. W. Mess, E. Lagendijk, and W. J. Huiskamp, Phys. Letters **25A**, 329 (1967).
[28] R. C. Sapp (unpublished).

TABLE VI. Calculated and experimental properties of lanthanum cobalt double nitrate. Only the X-X and X-Y nearest-neighbor interactions have been considered in the calculations except in the total ordering energy.

	Units	Calculated	Experimental
$C_{\parallel}$		2.879	2.893[a]
$C_{\perp}$		1.338	1.3167[a]
$(\theta_1)_{\parallel}$	°K	−0.296	−0.355[a]
$(\theta_2)_{\parallel}$	°K²	+0.065	+0.169[a]
$(\theta_1)_{\perp}$	°K	−0.110	−0.0723[a]
$(\theta_2)_{\perp}$	°K²	+0.00876	−0.0157[a]
		0.00900[b]	0.00855[a]
		0.01070[b]	0.01186[a]
b_M	°K²	0.0156	0.0152(0.0155)[c,d]
$\frac{E_{tot}}{R}$	°K	0.148	0.157[c]

[a] Selected for best fit of susceptibility with calculated values for other constants
[b] Reference 25. [c] Reference 30. [d] Reference 28.

We have considered two structures, the ferrimagnetic one described in the last paragraph and a very simple antiferromagnetic structure. In terms of layers, our antiferromagnetic structure consists of X-Y-X sandwiches as in the ferrimagnetic structure but with each successive sandwich oppositely oriented. In terms of a magnetic unit cell, that of the ferrimagnetic model is the same as the structural unit cell, X-Y-X along the c axis, with the spin orientations ↑-↓-↑. The antiferromagnetic structure requires a unit cell that is twice as long along the c axis containing the ions X-Y-X-X-Y-X with the spin orientations ↑-↓-↑-↓-↑-↓. An Ising model approximation in which the transverse components of the spin-spin interactions are ignored leads to a total ordering energy

$$E_{tot}^{(1)}=\tfrac{1}{3}N_0[6J_{00}(X,Y)\pm J_{00}(X,X)]=0.1546\text{R}\ \text{or}\ 0.1392\text{R}, \tag{73}$$

where the upper sign applies to the ferrimagnetic case and the lower applies to the antiferromagnetic case, and the former is favored by this result. The next step in the calculation is to evaluate the effects of the transverse components on the ordering energy. We have done this by using perturbation theory within the eigenstates of the Ising approximation. This method has been applied to the antiferromagnetic Heisenberg model,[29] but there it is clear that one must use very high orders of perturbation theory with the aid of diagrammatic analysis. Perturbation theory appears much more attractive in the present case because of the smallness of the transverse components. The off-diagonal element for the flipping of two X ion neighbors is only 8% of the excitation energy, and the corresponding ratio for the more numerous X-Y couplings is 5%. The result is that the first-order correction (second-order perturbation theory) is very small and

[29] H. L. Davis, Phys. Rev. **120**, 789 (1960).

the next order is quite negligible. The correction for either the ferrimagnetic or antiferromagnetic structure is

$$E_{tot}^{(2)}=0.0113\mathrm{R}, \quad (74)$$

which, added to (73), gives 0.1661R and 0.1505R with the ferrimagnetic state still favored, but the dipolar effects of more distant neighbors must be considered.

The Lorentz field is that given by the sum over all of the dipoles within a sphere and the contribution of the dipole moment per unit volume from the surface of the sphere, where it is assumed that the sphere is large enough that the continuum approximation is adequate outside the sphere. The field at an X or Y ion must be considered separately and the contributions from nearest-neighbor X-X and X-Y pairs omitted since those interactions have been incorporated in the preceding calculation. We designate the field from the dipole sum alone as $H^{(L)}$. For the ferrimagnetic array the contribution from the dipole sum may be written

$$E_{tot}^{(L)}=\tfrac{1}{3}N_0[2H_z^{(L)}(X)\mu_z(X)+H_z^{(L)}(Y)\mu_z(Y)]. \quad (75)$$

The same form is valid for the antiferromagnetic array since both the ionic moment and the field $H^{(L)}$ reverse for a translation by one of the basis vectors of the structural unit cell; but the values of $H_z^{(L)}$ are much different for the two cases. Evaluation of (75) by summing over a 100-A radius yields -0.0023R for the antiferromagnetic array and -0.02040R for the ferrimagnetic. For any sample shape there is no other contribution to the ordering energy of the antiferromagnet and we obtain 0.148R. For the ferrimagnetic array each dipole experiences a field of $\frac{1}{3}4\pi M$ in the direction of the magnetization which increases the ordering energy, and another field $-NM$ from the dipoles on the surface of the sample. For a single domain of spherical shape, these fields cancel and the net ordering energy is 0.146R, marginally less than for the antiferromagnetic case. However, a single needle-shaped domain is found to have an ordering energy of 0.149R, which suggest that domain formation could lead to a slightly lower energy for the ferrimagnetic array. In either case the calculated ordering energy is 6% lower than the experimental value. Some, perhaps all, of this discrepancy is surely due to cumulative errors in the spin-spin interaction measurements and the calorimetric work. We believe that the perturbation theory based on an Ising model representation is accurate, but the method could bear further scrutiny. As always in guessing the ordered structure, there exist the possibility of subtly different structures with lower energy.

Mess *et al.*[30] have recently found that LCN below its Néel point shows a positive magnetocaloric effect for weak fields along the symmetry axis, a behavior usually associated with ferri- or ferromagnetics. They also find that, although the susceptibility parallel to the symmetry axis falls off below the Néel point as expected for an antiferromagnet, there is a very sharp peak just at the Néel point. They have also noted that a large fraction of the spin entropy is removed above the Néel point, rather more than for a 6-neighbor Heisenberg model. The last of these properties correlates rather well with the dominance of the X-Y interaction. Within an X-Y-X sandwich there are only 4 bonds per spin; and, in isolation, this sandwich would order ferrimagnetically; but only after it had developed a large amount of short-range order. The development of long-range order may be precipitated by the combined effect of the X-X and dipolar interactions in a manner analogous to the effect of weak interchain interactions between Ising chains.[31] The X-X interactions favor ferrimagnetism, the dipolar effects antiferromagnetism; and the issue hangs in a precarious balance. It may be that the unorthodox behavior of the susceptibility and magnetocaloric effect are a consequence of the rather unusual bonding situation.

VI. SUMMARY AND CONCLUSIONS

The experimental results presented in this paper define the spin-spin interactions of Co^{2+} pairs in several diamagnetic double nitrates to an accuracy approaching 1%. The success with which the bulk properties of lanthanum cobalt double nitrate are explained by the measured pair interactions establishes the interactions to be the same in the concentrated material within the combined errors in the bulk properties and the pair measurements, about 5%. The investigation of the g factors in mixed crystals has established the proper g factors for LCN to be those measured for X-X pairs and isolated Y ions.

For the X-Y interaction, a plausible explanation has been given in terms of superexchange between orbitals. It is straightforward to extend this model to predict the X-Y interactions for combinations of Co^{2+}, Ni^{2+}, Mn^{2+}, and Cu^{2+} on the two sites. The situation for Cu^{2+} is a very interesting one because it involves a single e_g orbital and exhibits a static Jahn-Teller effect at low temperatures.[32] Some of these interactions can be studied with the pair technique, and others by measurements on concentrated materials. We believe that it is valid to generalize from the present study to conclude that only the nearest-neighbor X-X and X-Y interactions are nondipolar in the double nitrates. Assuming this, it is not possible in general to determine the interactions from the Weiss constants and the magnetic specific-heat tail unless special assumptions are made about the form of the nondipolar interaction. Fortunately, the orbital angular momentum effects in the

[30] K. W. Mess, E. Lagendijk, N. J. Zimmerman, A. J. Van Duyneveldt, J. J. Giesen, and W. J. Huiskamp, Physica **43**, 165 (1969).

[31] B. Bleaney, K. D. Bowers, and R. J. Trenam, Proc. Roy. Soc. (London) A228, 157 (1955).

[32] G. F. Newell and E. W. Montroll, Rev. Mod. Phys. **25**, 353 (1953).

ground states of Mn^{2+}, Cu^{2+} and Ni^{2+} are sufficiently small that the isotropic contribution to the superexchange will be dominant. The discussion in Sec. V shows that reliable Weiss constants are difficult to obtain, even from very good susceptibility data. In spite of this, the paramagnetic bulk properties are likely to be the most helpful guide since the diverse and sometimes complex behavior of LCuN, LNiN, LCoN, and LMnN reported by Mess *et al.*[30] appear to offer a considerable challenge even when the spin-spin interactions are known.

The X-X interaction is an example in which the structure does not suggest a simple model for the superexchange. The presence of a threefold axis provides some simplification, and it appears that the intercomparison of a number of ions could lead to fruitful results. Unfortunately, the experimental situation for pair studies is much more tedious for the X-X pairs than for the X-Y pairs. It should be noted that the circumstance which causes the interaction to be weak for such a small interionic separation is the lack of transfer between orbitals for symmetry reasons. This is the situation in which ferromagnetic potential exchange is likely to be competitive with kinetic exchange.

The ubiquity of hydrogen bonding in hydrated paramagnetic salts leads us to suggest that the e_g orbitals at the end of hydrogen bonds may be of very general importance in such materials. It is possible that approaches motivated in this way will contribute to a coherent and compact description of interactions which exhibit a vast diversity in the effective spin formulation.

ACKNOWLEDGMENTS

We are grateful to K. W. Mess for informing us of the results obtained at Leiden in advance of publication. One of us (D. P. S.) wishes to acknowledge a NASA fellowship held during the early part of this work. The other (J. W. C.) gratefully acknowledges support from the Guggenheim Foundation that made a part of this work possible. The same author is also indebted to Professor Bleaney for the hospitality of the Clarendon Laboratory while this work was concluded, and to him as well as Dr. J. M. Baker for stimulating discussions.

APPENDIX

The g tensor can always be made symmetrical in the indices by a suitable choice of the effective spin operator. In the description of the perturbative effects of strain, it is best to keep the definition of the effective spin fixed and to characterize the effects by a change in the g tensor that may not be symmetrical. The change in the Zeeman splitting that is induced by the strain is given by the change in the effective g tensor which has been denoted simply as g in Sec. II and is related to the changes in the components of the g tensor by

$$\delta g=(\mathbf{H}\cdot\delta\mathbf{g})\cdot(\mathbf{H}\cdot\mathbf{g})/gH^2 \tag{A1}$$

or

$$\delta g=\frac{1}{2g}\sum_{ij}(\delta g_{ij}g_{jj}+\delta g_{ji}g_{ii})l_il_j=\sum_{ij}f_{ij}l_il_j, \tag{A2}$$

where l_i and l_j denote the direction cosines of the applied field, and it has been assumed that the axes are those which diagonalize the unperturbed g tensor. The Zeeman shifts are therefore sensitive only to the symmetrized quantity f_{ij}.

For the special case in which the magnetic field is perpendicular to the symmetry axis, so that $g_{xx}=g_{yy}$, the upward and downward shifts of the pair spectrum are given by

$$H_\pm=a_g+a_2\pm a_s+(b_g+b_2\pm b_s)\cos2\phi+(c_g+c_2\pm c_s)\sin2\phi, \tag{A3}$$

where

$$a_g=\tfrac{1}{2}(f_{xx}+f_{yy}),\quad b_g=\tfrac{1}{2}(f_{xx}-f_{yy}),\quad c_g=f_{xy}, \tag{A4}$$

$$a_s=-J_{1-1}\cos\phi_{1-1},\quad b_s=J_{11}\cos\phi_{11},\quad c_s=J_{11}\sin\phi_{11}, \tag{A5}$$

and a_2, b_2, and c_2 are second-order effects which must be calculated. As noted in Sec. II, the g shifts and second-order effects can be separated by their frequency dependence; they do not contribute to the separation ΔH if the upper and lower components are properly identified. The phase of the oscillation of the upper and lower components is $(2\psi_\pm+\phi_{11})$, and

$$\tan(2\psi_\pm+\phi_{11})=-(c_g+c_2\pm c_s)/(b_g+b_2\pm b_s). \tag{A6}$$

It is quite possible to make a major error in the identification of high- and low-field components if the difference in phase is 60° or more. Measurements at several frequencies are necessary to guard against such an error.

For Co^{2+} in LZN, $\phi_{11}=0$ (with the choice of signs chosen in our Table III), so $c_s=0$; the second-order contribution c_2 is also zero; and $b_s\gg b_g$, b_2. The phase shift of the upper spectra relative to the lower then gives a very accurate measure of f_{xy};

$$\tan2\psi_+-\tan2\psi_-=-2f_{xy}h\nu/g_1J_{11}. \tag{A7}$$

Upper limits on the value of f_{xz} and f_{yz} were established by a study of the X-Y spectrum near the symmetry axis. As described in Sec. III and illustrated in Figs. 4, 7, and 8, the components of intensity one separate from those of intensity two as the angle from the symmetry axis is increased. This is because there are two distinct values of ϕ, 0 and ±120°. Likewise, f_{xz} and f_{yz} produce a centroid shift that is ϕ-dependent. The separation of the spectra from the isolated reference is given by

$$H_\pm=\pm J_{00}'/2g\beta+(h\nu/g^2\beta)(\sin\theta\cos\theta)\times(f_{xz}\cos\phi+f_{yz}\sin\phi) \tag{A8}$$

plus a second-order correction. One effect of this is that when the two components of the high-field spectrum are separated by an integral number of hyperfine intervals so to appear rather simple, the low-field spectrum will not show such simplifications. This effect can be observed at our largest values of θ (30°) and 37 GHz. Some of the effect arises from second-order contributions of the spin-spin interaction; without a very laborious analysis which the data hardly justifies. it is only possible to place upper limits on f_{xz} and f_{yz}.

PHYSICAL REVIEW VOLUME 187, NUMBER 2 10 NOVEMBER 1969

Theory of Magnetic Relaxation in a Near-Ising System: DyES†

PETER M. RICHARDS
Department of Physics, University of Kansas, Lawrence, Kansas 66044
(Received 11 June 1969)

A theory of magnetic relaxation in an Ising system is developed, and the results are compared with the experiments of Cooke, Edmonds, Finn, and Wolf on dysprosium ethyl sulfate (DyES), believed to be an Ising dipolar ferromagnet below 0.13°K. Small spin-spin perturbations are postulated to give rise to relaxation within the spin system without having to invoke spin-lattice coupling. The methods of Kubo and Tomita are used to express the relaxation rate in terms of time correlation functions. These can be evaluated far more easily in an Ising system than in a Heisenberg one, and what appear to be reliable estimates are made for the DyES lattice. The resulting relaxation rate is strongly dependent on the spontaneous magnetization, which is calculated from a phenomenological model simlar to the one employed by Cooke *et al.* (nearest-neighbor Ising linear chain plus molecular field). Good agreement is then obtained with experiment for temperature dependence of the ferromagnetic relaxation time. Numerical agreement requires either a strain-induced $g_\perp$ of about 0.05 or a next-nearest-neighbor spin-spin interaction of about 2×10^{-4} cm^{-1}. These are shown to be plausible numbers by investigating effects of rhombohedral lattice distortion and electric quadrupole-quadrupole interaction.

I. INTRODUCTION

THE Ising-model Hamiltonian

$$\mathcal{H}_0=-\tfrac{1}{2}\hbar\sum_{ij}J_{ij}S_i^zS_j^z, \qquad (1)$$

which couples only longitudinal components of spin operators $\mathbf{S}_i$ and $\mathbf{S}_j$ on lattice sites i and j, has received considerable attention in discussing thermodynamic properties of ferromagnetism. It may be handled with much greater ease than the isotropic Heisenberg Hamiltonian, and this advantage often outweighs the fact that the Heisenberg model generally comes much closer to describing physical systems. In recent years, interest in the Ising model has been heightened by the discovery of compounds for which interactions are highly anisotropic and do conform to (1). Dysprosium ethyl sulfate (DyES) is an excellent example.[1] Here the interactions are largely dipolar, and the highly anisotropic g tensor ($g_{\parallel}=10.8$, $g_\perp\approx0$) reduces the dipolar Hamiltonian to the form (1), in which z is the direction of the crystalline c axis along which $g_{\parallel}$ is measured.

Cooke, Edmonds, Finn, and Wolf,[2,3] hereafter referred to as CEFW, have reported measurements of magnetic relaxation times as well as static properties in DyES below the Curie temperature of about 0.13°K. Their work represents the first study of ferromagnetic relaxation in a system whose dominant Hamiltonian is Ising-like. It is the purpose of this paper to investigate the theory of magnetic relaxation in a near-Ising system and make comparison with the experimental results of CEFW. This problem is of particular interest since the necessary time correlation functions can be computed with much more reliability than for the Heisenberg model. Thus it should be possible to obtain meaningful comparison between theory and experiment with a minimum number of assumptions.

The term "near Ising" requires some clarification. CEFW measure relaxation of the total z component (which is the only component if $g_\perp=0$) of magnetization M_z, which is proportional to $\sum_j S_j^z$. It is evident that M_z commutes with $\mathcal{H}_0$ as given by (1), so that no relaxation is possible if the total Hamiltonian is given solely by the Ising term. There are two possible modifications to (1) which can produce relaxation. First, one may consider spin-lattice relaxation due to coupling between a spin $\mathbf{S}_i$ and lattice vibrations. We dismiss this at the outset for the following reason. A striking feature of the results of CEFW which any theory must explain is the shortness of the relaxation times. At 0.125°K they measure a time of about 2×10^{-6} sec. As they note, it is

† Supported by the U. S. Atomic Energy Commission. Portions of this work were reported in Bull. Am. Phys. Soc. **14**, 408 (1969).
[1] A. H. Cooke, D. T. Edmonds, C. B. P. Finn, and W. P. Wolf, Proc. Roy. Soc. (London) **A252**, 246 (1959).
[2] A. H. Cooke, D. T. Edmonds, C. B. P. Finn, and W. P. Wolf, Proc. Roy. Soc. (London) **A306**, 313 (1968).
[3] A. H. Cooke, D. T. Edmonds, C. B. P. Finn, and W. P. Wolf, Proc. Roy. Soc. (London) **A306**, 335 (1968).